Yu *et al. Genome Biology* (2024) 25:307
https://doi.org/10.1186/s13059-024-03448-8

Genome Biology

RESEARCH Open Access

Systemic evaluation of various CRISPR/Cas13 orthologs for knockdown of targeted transcripts in plants

Lu Yu[1], Jiawei Zou[1], Amjad Hussain[1], Ruoyu Jia[1], Yibo Fan[1], Jinhang Liu[1], Xinhui Nie[2], Xianlong Zhang[1] and Shuangxia Jin[1*]

*Correspondence: jsx@mail.hzau.edu.cn

[1] Hubei Hongshan Laboratory, National Key Laboratory of Crop Genetic Improvement, Huazhong Agricultural University, Wuhan 430070, China
[2] Key Laboratory of Oasis Ecology Agricultural of Xinjiang Production and Construction Corps, Agricultural College, Shihezi University, Shihezi 832003, Xinjiang, China

Abstract

Background: CRISPR/Cas13 system, recognized for its compact size and specificity in targeting RNA, is currently employed for RNA degradation. However, the potential of various CRISPR/Cas13 subtypes, particularly concerning the knockdown of endogenous transcripts, remains to be comprehensively characterized in plants.

Results: Here we present a full spectrum of editing profiles for seven Cas13 orthologs from five distinct subtypes: VI-A (LwaCas13a), VI-B (PbuCas13b), VI-D (RfxCas13d), VI-X (Cas13x.1 and Cas13x.2), and VI-Y (Cas13y.1 and Cas13y.2). A systematic evaluation of the knockdown effects on two endogenous transcripts (*GhCLA* and *GhPGF* in cotton) as well as an RNA virus (TMV in tobacco) reveals that RfxCas13d, Cas13x.1, and Cas13x.2 exhibit enhanced stability with editing efficiencies ranging from 58 to 80%, closely followed by Cas13y.1 and Cas13y.2. Notably, both Cas13x.1 and Cas13y.1 can simultaneously degrade two endogenous transcripts through a tRNA-crRNA cassette approach, achieving editing efficiencies of up to 50%. Furthermore, different Cas13 orthologs enable varying degrees of endogenous transcript knockdown with minimal off-target effects, generating germplasms that exhibit a diverse spectrum of mutant phenotypes. Transgenic tobacco plants show significant reductions in damage, along with mild oxidative stress and minimal accumulation of viral particles after TMV infection.

Conclusions: In conclusion, our study presents an efficient and reliable platform for transcriptome editing that holds promise for plant functional research and future crop improvement.

Keywords: Plants, CRISPR/Cas13 orthologs, RNA targeting, Transcript decay (gene knockdown), RNA virus interference

Background

The Clustered Regularly Interspaced Short Palindromic Repeats (CRISPR)-associated protein (Cas) system has been engineered as a robust genome-editing tool, enabling efficient manipulation of microbial, mammalian, and plant genomes. Current genome

editing tools, particularly those utilizing programmable nucleases like CRISPR/Cas9, have been extensively adopted for targeted DNA cleavage. RNAs, including mRNA, lncRNA, and circular RNA, fulfill significant and diverse roles in biological processes. A variety of methodologies have been developed to investigate the biological roles of gene or RNA downregulation, including antisense RNAs, ribozymes, RNA interference (RNAi), and CRISPR interference (CRISPRi). Nonetheless, these approaches face several challenges related to efficiency, specificity, toxicity, and delivery [1]. RNAi is widely used to modulate RNA stability by recognizing small interfering RNAs (siRNAs) [2–4]. However, RNAi exhibits reduced effectiveness against nuclear RNAs and is often linked to a high incidence of off-target effects, as well as genetic instability [5, 6]. The CRISPRi system comprises dead Cas9 (dCas9) in conjunction with transcriptional repressor proteins, which are directed by guide RNA (gRNA) to specifically target promoter regions and inhibit transcription. This system functions under the constraints of protospacer adjacent motif (PAM) requirements and is also influenced by the background expression levels of the target gene [7]. Although off-target effects can occur in CRISPRi systems, they are considerably less frequent than those associated with RNAi, primarily due to the proximity of the CRISPRi complex to the transcription start site (TSS) [8]. Consequently, current transcriptome editing tools for targeting RNA to regulate or manipulate gene expression remain limited.

Recently, CRISPR/Cas13, a novel RNA-guided RNA-targeting CRISPR/Cas system, has been engineered to cleave RNA targets carrying complementary protospacers [9]. Cas13 proteins exhibit two distinct RNase activities: the processing of precursor CRISPR RNA (pre-crRNA) into mature crRNA, and the degradation of target RNA mediated by two Higher Eukaryotes and Prokaryotes Nucleotide-binding (HEPN) domains. Cas13 proteins enable precise RNA binding and cleavage, exhibiting a preference for targets that include protospacer flanking sites (PFS), as evidenced in both bacterial and mammalian cells [10–13]. Studies have shown that two HEPNs can form catalytic sites for RNase activity (termed collateral activity) on the protein surface when Cas13 binds to the target RNA. This interaction may result in the hybrid cleavage of bystander RNAs, in addition to the specific cleavage of target RNAs [14, 15]. Collateral activity fundamentally differs from traditional off-target effects. Off-target effects are largely independent of the presence of the intended on-target, whereas collateral activity is activated only upon recognition of on-target RNA that perfectly matches the crRNA [16]. In principle, conventional off-targets can also trigger collateral activity, provided that the mismatch is tolerated. Notably, substantial variation in collateral activity has been observed among different subtypes of Cas13 proteins within mammalian cells [17]. Intriguingly, the extent of collateral activity also varies across different cell types [18]. Therefore, different subtypes of Cas13 may exhibit variations in editing efficiency and characteristics across both plant and mammalian cells. It is particularly crucial to investigate whether distinctions exist between these two cell types.

Based on phylogenetic analysis, the Cas13 family is currently classified into 11 subtypes: Cas13a, Cas13b, Cas13c, Cas13d, Cas13e, Cas13f, Cas13g, Cas13h, Cas13i, Cas13x, and Cas13y [10, 11, 19–23]. Although all Cas13 systems function as RNA-guided RNases, they exhibit differences in protein size, structure, and efficiency within eukaryotic cells. The positioning of HEPN domains, the length of the crRNA, and the

spacer sequence differ depending on the specific type of Cas13 protein. In Cas13a, Cas13c, and Cas13d, HEPN domains are located at both the center and the C-terminus [10]. In contrast, for Cas13b, Cas13x, and Cas13y, HEPN domains are situated at the extreme N-terminus and C-terminus of the linear protein [19, 22]. Moreover, the direct repeat (DR) sequences of Cas13b, Cas13x, and Cas13y are positioned at the 5' end with an orientation that contrasts with those observed in other subtypes. Among various Cas13 systems, Cas13a, Cas13b, and Cas13d are the most widely used in mammalian cells.

Cas13a is the first characterized subtype of the Cas13 family, with LshCas13a derived from *Leptotrichia shahii* recognized for its ability to cleave single-stranded RNA (ssRNA) [10, 24]. In contrast, Cas13a from *Leptotrichia wadei* (LwaCas13a) demonstrates more potent RNA-targeting activity than LshCas13a [25]. Notably, Cas13b is distinctive among type VI CRISPR effectors due to its linear domain architecture and the specific positioning of the DR sequence. It exhibits superior efficacy compared to LwaCas13a and does not require a stabilizing protein for its activity in mammalian cells [24]. Cas13c remains the least functionally characterized and shows lower efficiency in RNA targeting compared to Cas13a, Cas13b, and Cas13d [26]. Cas13d, including RfxCas13d from *Ruminococcus flavefaciens*, shows minimal sequence similarity to previously characterized Cas13 nucleases. The median size of Cas13d proteins ranges from 190 to 300 amino acids, which is approximately 26% smaller than that of the previously reported Cas13a, Cas13b, and Cas13c proteins [7, 20]. It is recognized for its versatility and robust activity, and does not impose PFS constraints—unlike earlier Cas13 nucleases in mammalian cells [26–28]. Recently identified subfamilies of Cas13 include Cas13x and Cas13y; notably, the Cas13x.1 protein is approximately 200 amino acids smaller than RfxCas13d [22]. It possesses capabilities for RNA knockdown, RNA repair, and RNA splicing [29–32], all of which can be encapsulated within *Adeno-associated viruses* (AAVs) vectors. CRISPR/Cas13 systems show enhanced catalytic activity and specificity, facilitating a wide range of applications across diverse organisms [32–35].

In mammalian cells, CRISPR/Cas13 has been shown to effectively inhibit both nuclear and cytoplasmic RNAs, as well as viral RNAs [7, 36, 37]. In plants, recent studies on CRISPR/Cas13 systems have mainly focused on viral RNA interference, including *Turnip mosaic virus* (TuMV) [27, 28, 38], *Potato virus Y* (PVY) [35], *Tomato spotted wilt virus* (TSWV) [39], *Tobacco mosaic virus* (TMV) [40], *Southern rice black-streaked dwarf virus* (SRBSDV) [40], *Sweet potato virus disease* (SPVD) [41], *Grapevine virus A* (GVA) [42], and *Rice stripe mosaic virus* (RSMV) [40]. The evaluation of Cas13-mediated endogenous mRNA knockdown has been reported in a limited number of studies involving plants, primarily focusing on the Cas13a subtype. LwaCas13a effectively facilitated the knockdown of three endogenous transcripts: 5-enolpyruvylshikimate-3-phosphate synthase (EPSPS), hydroxycinnamoyl transferase (HCT), and phytoene desaturase (PDS) in rice protoplasts [25]. Successful knockdown of PDS transcripts in *Nicotiana benthamiana*, *Arabidopsis thaliana*, and *Solanum lycopersicum* was achieved using LbaCas13a and LbuCas13a via *Agrobacterium* infiltration [43]. It is regrettable that various Cas13 orthologs from different subtypes, which are prevalent in mammalian cells, have not yet been characterized in plant systems. Recent studies have highlighted the collateral activity and toxic effects associated with Cas13 proteins, which can lead

to adverse side effects in mammalian cells and organisms [17, 30, 44–46]. Nonetheless, there is currently a lack of reports exploring the editing efficiency, potential toxicity, and off-target effects of Cas13 subtypes for the knockdown of endogenous transcripts in plants. Identifying Cas13 nucleases that exhibit elevated safety, specificity, and editing efficacy is a primary objective in advancing plant RNA targeting technologies, which is essential for broadening their potential applications in plants.

In this study, we present a full spectrum of the editing profiles of seven Cas13 orthologs from five subtypes: VI-A (LwaCas13a), VI-B (PbuCas13b), VI-D (RfxCas13d), VI-X (Cas13x.1 and Cas13x.2), and VI-Y (Cas13y.1 and Cas13y.2). This represents the first report detailing the PbuCas13b, Cas13x.1, Cas13x.2, Cas13y.1, and Cas13y.2 systems in plants. A systematic evaluation of the knockdown effects on two endogenous transcripts (*GhCLA* and *GhPGF* in cotton) and an RNA virus (TMV in tobacco) revealed that RfxCas13d, Cas13x, and Cas13y exhibited superior and more stable editing efficiencies, followed by PbuCas13b, while LwaCas13a demonstrated the lowest efficiency. Notably, both Cas13x.1 and Cas13y.1 exhibit the capability to simultaneously knockdown two endogenous transcripts with high efficacy using a tRNA-crRNA cassette approach. All Cas13 orthologs significantly enhanced resistance to TMV in transgenic tobacco plants. This study systematically evaluates and characterizes the effectiveness and utility of various Cas13 orthologs in plants, providing a valuable approach for analyzing gene function and is expected to facilitate future crop improvement.

Results

Designing and engineering various CRISPR/Cas13 systems for *in planta* expression

The selection of Cas13 orthologs was based on the intensity of RNA-editing activity reported both in vitro and in mammalian cells. The spatial structures of the selected proteins were predicted using AlphaFold, revealing that these proteins exhibit significantly different spatial conformations. LwaCas13a (VI-A), PbuCas13b (VI-B), and RfxCas13d (VI-D) possess more compact structures compared to Cas13y.2 (VI-Y). Interestingly, Cas13x.1 (VI-X), Cas13x.2 (VI-X), and Cas13y.1 (VI-Y) display substantial differences in their amino acid sequences, accompanied by relatively flexible spatial conformations (Additional file 1: Fig. S1a). Therefore, these Cas13 orthologs were selected for a comprehensive assessment of their editing efficiency and catalytic activities in RNA degradation within plant systems.

To engineer binary vectors for *in planta* expression of CRISPR/Cas13 orthologs, we codon-optimized the nucleotide sequences of LwaCas13a, PbuCas13b, RfxCas13d, Cas13x.1, Cas13x.2, Cas13y.1, and Cas13y.2 based on plant genomics characteristics. Each Cas13 ortholog was co-delivered with position-matched crRNAs and their corresponding DR sequences to ensure effective targeting in plants (Fig. 1a). Cas13 orthologs were assembled using unique restriction enzymes to generate full-length clones flanked by attL1 and attL2 recombination sites. It has been demonstrated that nuclear localization signals (NLS) can significantly enhance the knockdown activity of Cas13x [22]. Therefore, two types of NLS were fused to both the C-terminus and N-terminus of the Cas13 protein. All *Cas13* genes were driven by the *pOSUbi10* promoter, while crRNA transcription was facilitated by the endogenous type III promoter *pGhU6-7* derived from cotton, in accordance with our recent studies [47, 48] (Fig. 1b).

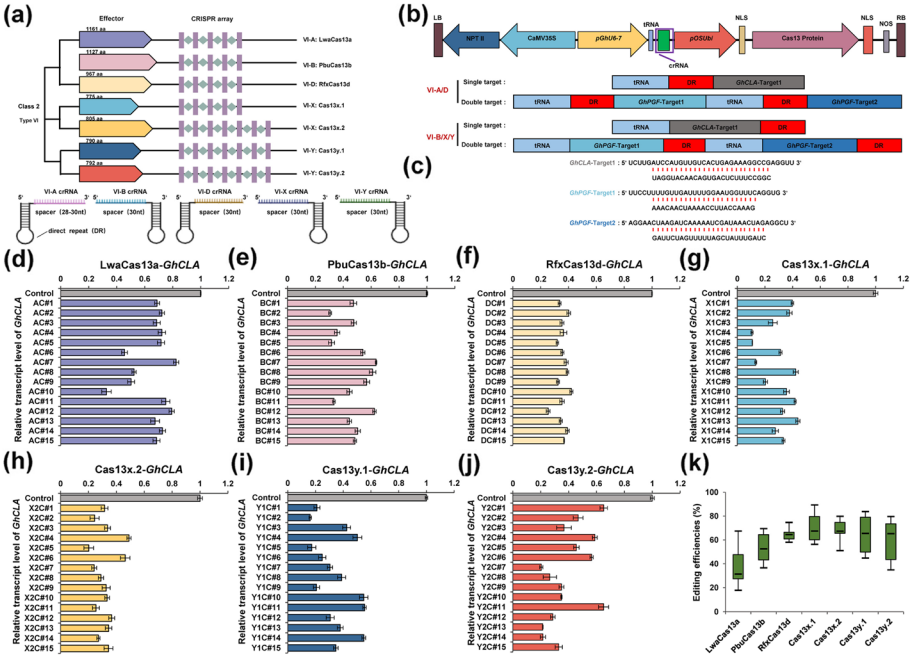

Fig. 1 Programmable design and efficiency assessment of various Cas13 orthologs in cotton. **a** Structural representations of various Cas13 orthologs and their corresponding crRNA structures. aa: amino acid. **b** Schematic representation of a multi-guide expression cassette design to target the endogenous transcripts *GhCLA* and *GhPGF*. **c** Sequence information of the target transcripts for different Cas13 proteins. **d-j** Transcript levels of the *GhCLA* gene in transgenically edited plants expressing the LwaCas13a, PbuCas13b, RfxCas13d, Cas13x.1, Cas13x.2, Cas13y.1, and Cas13y.2 systems, respectively. Regenerated plants were assigned numerical identifiers based on the classification of Cas13 protein subfamilies and the target gene *GhCLA*. For instance, the label AC# indicates T_0 generation plants that underwent LwaCas13a-mediated knockdown of the *GhCLA* gene, while the corresponding T_1 generation is designated as AC#L. **k** Comparison of the knockdown efficiency of *GhCLA* transcripts mediated by different Cas13 orthologs in several T_0 regenerated plants. Error bars represent the mean ± S.D. ($n = 3$)

The *GhCLA* (*Chloroplastos alterados*) gene, plays a crucial role in chloroplast development. Previous studies have shown that knockout mutants of this gene exhibit an albino phenotype [49, 50]. Additionally, silencing the *GhPGF* (*Pigment gland formation*) gene through RNAi, CRISPR/Cas9 or CRISPR/Cas12 results in a glandless phenotype [51–53]. In contrast to the complete knockout strategy enabled by CRISPR/Cas9, we propose that utilizing the CRISPR/Cas13-mediated knockdown approach targeting the *GhCLA* and *GhPGF* genes may yield plants with milder mutant phenotypes, such as chlorophyll loss and a reduced number of glands. Consequently, the two endogenous genes *GhCLA* and *GhPGF* were selected as target transcripts to evaluate the editing efficiency of various CRISPR/Cas13 systems. Tissue-specific expression was observed for both transcripts, revealing a statistically significant difference in RNA abundance between them (Additional file 1: Fig. S1b). A previous study indicated that the tRNA-gRNA transcription unit can enhance gRNA transcription within the CRISPR/Cas system for plant genetic editing [48, 53]. Therefore, a specific crRNA (crRNA-T) was designed to target *GhCLA*, leading to the construction of seven targeted vectors utilizing the tRNA-crRNA T transcription unit. In addition, two crRNAs (crRNA-T1 and crRNA-T2) were developed to target *GhPGF*, resulting in seven additional vectors created using the tRNA-crRNA T1-tRNA-crRNA T2 strategy (Fig. 1c & Additional file 2: Table S1). *Agrobacterium*-mediated

transformation was applied to introduce T-DNA containing different *Cas13* genes and crRNAs into the cotton plant genome (Additional file 1: Fig. S1c).

Cas13 orthologs efficiently facilitated the degradation of *GhCLA* transcripts using a single crRNA in cotton

Through *Agrobacterium*-mediated transformation, a substantial number of independently regenerated plants were obtained that harbor Cas13 systems specifically targeting the *GhCLA* gene using a single crRNA. For each Cas13 system, more than 15 positive T_0 plants were selected to measure the transcript levels of target genes (Additional file 2: Table S2). Regenerated plants were assigned numerical identifiers according to the classification of Cas13 protein subfamilies and their target gene. For instance, the label AC# indicates T_0 generation plants that underwent LwaCas13a-mediated knockdown of the *GhCLA* gene, while the corresponding T_1 generation is designated as AC#L. Seven *Cas13* genes exhibited well transcription across all T_0 plants, as confirmed by quantitative reverse transcription PCR (qRT-PCR) (Additional file 1: Fig. S2). To assess the efficacy of the CRISPR/Cas13 systems in degrading targeted mRNA using a single crRNA, qRT-PCR was performed to measure the transcript levels of *GhCLA*. The decrease in transcript abundance is quantified as the editing efficiency of the Cas13 systems.

It was observed that the transcript levels of *GhCLA* were specifically downregulated in all T_0 plants, while the control (non-crRNA vector) remained unchanged. The average transcript levels of *GhCLA* in LwaCas13a-edited plants decreased to 65.3%, with plant #10 (designated as AC#10) exhibiting the lowest recorded level at 32.7% (Fig. 1d). In contrast, the average transcript levels mediated by PbuCas13b declined to 47.4%, with the lowest level found in plant #11 (designated as BC#11), which reached 30.5% (Fig. 1e). The mRNA transcript levels were significantly downregulated in RfxCas13d-edited plants, ranging from 30 to 40%, with a notable decrease of 25.4% observed in plant #12 (designated as DC#12) (Fig. 1f). Notably, the average transcript levels of *GhCLA* in edited plants mediated by Cas13x.1, Cas13x.2, Cas13y.1, and Cas13y.2 were measured at 29.8%, 32.1%, 35.3%, and 39.7%, respectively (Fig. 1g-j).

In conclusion, CRISPR/Cas13 systems possess the capability to target and knockdown *GhCLA* transcripts using a single crRNA. The average editing efficiencies were 34.7% for LwaCas13a, 52.6% for PbuCas13b, 64.3% for RfxCas13d, 70.2% for Cas13x.1, 67.9% for Cas13x.2, 64.7% for Cas13y.1, and 60.3% for Cas13y.2 (Fig. 1k). Notably, the editing efficiency of LwaCas13a has been reported to range from 58 to 88% in mammalian cells, exceeding 50% and reaching as high as 78% in rice protoplasts [25]. However, our study revealed that the editing efficiency of LwaCas13a was significantly lower in stably edited plants, with most efficiencies concentrated between 30 and 50%. A comprehensive assessment of multiple CRISPR/Cas13 nucleases confirmed that RfxCas13d, Cas13x, and Cas13y possess superior editing efficiencies along with enhanced stability, followed by PbuCas13b. In contrast, LwaCas13a exhibited the lowest level of mRNA decay activity. These findings indicate that all tested CRISPR/Cas13 orthologs are capable of performing targeted mRNA decay to modulate gene expression in cotton; however, variations in editing efficiency were observed.

Efficient degradation of *GhCLA* transcripts leads to a chlorophyll fading phenotype that is faithfully inherited to T_1 progeny

Several independent T_0 cotton plants, including AC#8 (plant #8 of LwaCas13a-*GhCLA*), BC#1 (plant #1 of PbuCas13b-*GhCLA*), DC#1 (plant #1 of RfxCas13d-*GhCLA*), X1C#1 (plant #1 of Cas13x.1-*GhCLA*), X2C#1 (plant #1 of Cas13x.2-*GhCLA*), Y1C#1 (plant #1 of Cas13y.1-*GhCLA*) and Y2C#2 (plant #2 of Cas13y.2-*GhCLA*), exhibited a distinct phenotype characterized by chlorophyll fading throughout the entire plant (Fig. 2a). These plants displayed varying degrees of chlorophyll fading during the genetic transformation process, which may be attributed to differences in cleavage efficiency among the various Cas13 orthologs. The chlorophyll content extracted and quantified from the leaves of T_0 seedlings revealed significant reductions of 32%, 46%, 60%, 65%, 68%, 70%, and 68% for AC#8, BC#1, DC#1, X1C#1, X2C#1, Y1C#1, and Y2C#2, respectively, in comparison to control plants (Fig. 2b). This decline in chlorophyll content was consistent with the observed reduction in transcript levels of the *GhCLA* gene.

To evaluate the potential inheritance of Cas13-mediated knockdown in the germline to T_1 progeny, we assessed the editing efficiency of T_1 generations. All nomenclature for the T_0 and T_1 generations exhibits systematic consistency; specifically, the T_0 generation is designated as AC#1, while its corresponding T_1 generation is labeled as AC#L1.

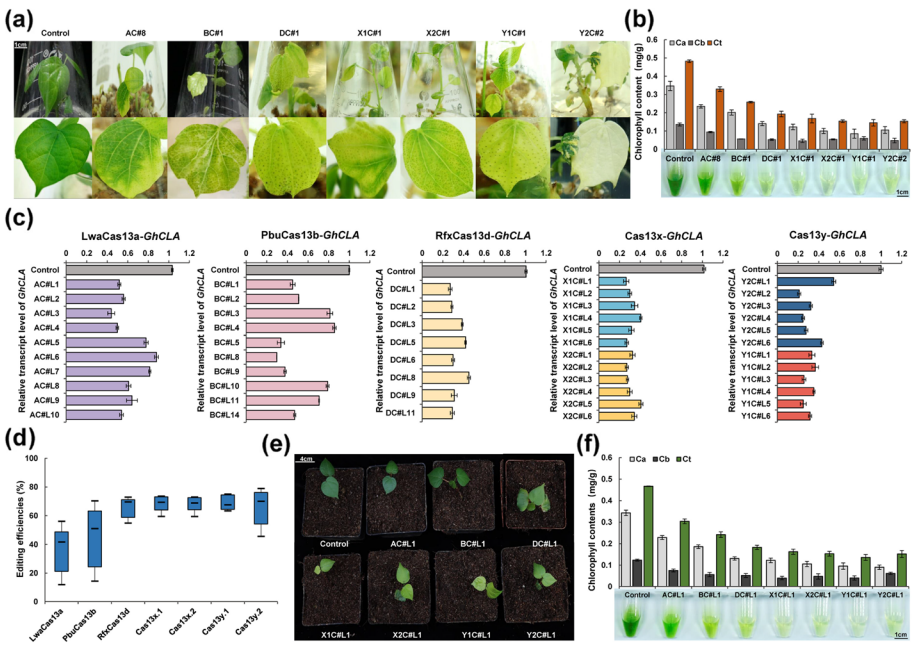

Fig. 2 Editing efficiency and phenotypes of various Cas13 orthologs targeting *GhCLA* transcripts with a single crRNA. **a** Chlorophyll fading phenotypes of T_0 Cas13-edited plants during *Agrobacterium*-mediated transformation. Bars, 1 cm. **b** Chlorophyll content in the leaves of transgenic plants, with representative wells containing chlorophyll extract shown below (in green). Ca: chlorophyll a; Cb: chlorophyll b; Ct: total chlorophyll. Bars, 1 cm. **c** Transcript levels of the *GhCLA* gene in T_1 plants expressing the LwaCas13a, PbuCas13b, RfxCas13d, Cas13x.1, Cas13x.2, Cas13y.1, and Cas13y.2 systems, respectively. **d** Comparison of knockdown efficiency for *GhCLA* transcripts mediated by various Cas13 orthologs in T_1 plants. **e** Chlorophyll fading phenotypes of T_1 seedlings. Bars, 4 cm. **f** Quantification of chlorophyll in 4-week-old T_1 seedlings, with representative wells containing chlorophyll extract shown below (in green). Error bars represent the mean ± S.D. ($n = 3$). Bars, 1 cm

Seedlings were cultivated in a nutrient solution until they reached the second true leaf stage. More than 10 positive T_1 lines for each CRISPR/Cas13 ortholog were identified through molecular detection, confirming that *Cas13* genes were well and consistently transcribed (Additional file 1: Fig. S3). An analysis of target transcripts revealed that transcript levels of the *GhCLA* gene were specifically downregulated in selected T_1 plants, whereas the control levels remained unchanged (Fig. 2c). The average editing efficiencies were 37.3%, 44.0%, 66.0%, 68.0%, 68.4%, 68.8%, and 66.2% for LwaCas13a, PbuCas13b, RfxCas13d, Cas13x.1, Cas13x.2, Cas13y.1, and Cas13y.2, respectively (Fig. 2d). These results showed a consistent trend with the editing efficiencies observed in T_0 plants. Phenotypic analysis of 4-week-old T_1 seedlings, along with chlorophyll measurements of the second true leaf, revealed that seedlings harboring different Cas13 orthologs exhibited varying degrees of discoloration (Fig. 2e & f). These findings suggest that RNA degradation mediated by these Cas13 systems, along with the resulting phenotypes, can be reliably inherited from T_0 parental plants to their T_1 progeny.

Cas13 orthologs utilize two crRNAs to effectively downregulate *GhPGF* transcripts

Transgenic plants expressing Cas13 orthologs targeting the *GhPGF* gene were generated via *Agrobacterium*-mediated transformation (Additional file 2: Table S3). More than 10 positive T_0 plants exhibiting well-expressed Cas13 proteins for each Cas13 system were screened to evaluate editing efficiency (Additional file 1: Fig. S4). Regenerated plants were assigned numerical identifiers based on the classification of Cas13 protein subfamilies and their target gene. For instance, the label AP# indicates T_0 generation plants that underwent LwaCas13a-mediated knockdown of the *GhPGF* gene, while the corresponding T_1 generation is designated as AP#L. The results indicated that the transcript levels of *GhPGF* were specifically downregulated in the selected transgenic plants compared to control plants. Average decreases in *GhPGF* transcript levels were observed at 51.3%, 42.1%, 32.3%, 29.1%, 31.0%, 33.0%, and 34.0% for LwaCas13a, PbuCas13b, RfxCas13d, Cas13x.1, Cas13x.2, Cas13y.1, and Cas13y.2, respectively (Fig. 3a-3g). Consistent with the editing effects noted on the *GhCLA* gene, RfxCas13d, Cas13x, and Cas13y demonstrated significantly higher efficiencies in degrading the *GhPGF* gene, followed by PbuCas13b and LwaCas13a (Fig. 3h). These findings further corroborate that all Cas13 systems can accurately and stably cleave targeted mRNAs using a dual-crRNA cassette approach, thereby effectively downregulating gene expression.

Downregulation of *GhPGF* transcripts using CRISPR/Cas13 orthologs results in a reduced gland phenotype in cotton

Several T_0 positive plants, effectively edited with Cas13 orthologs targeting *GhPGF*, underwent phenotypic characterization. The total number of gossypol glands in the edited plants was reduced to varying degrees compared to control plants; however, no other significant phenotypic differences were observed (Fig. 3i). A notable reduction in the number of gossypol glands on cotton bolls was evident in the Cas13-edited plants (Fig. 3j). The number of gossypol glands on the cotton bolls decreased by 30.9%, 38.3%, 49.4%, 55.6%, 51.9%, 50.6%, and 53.1% for the plants designated as AP#3, BP#2, DP#3, X1P#2, X2P#3, Y1P#4, and Y2P#3, respectively (Fig. 4a). To more accurately assess the impact of reduced *GhPGF* transcripts, we quantified the

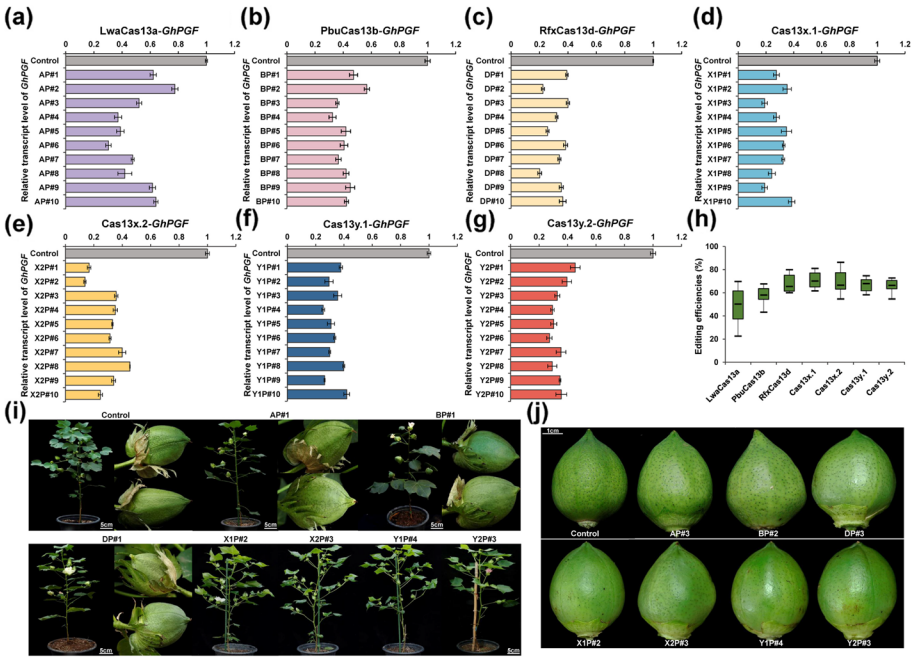

Fig. 3 Various Cas13 orthologs utilize two crRNAs to effectively downregulate *GhPGF* transcripts. **a-g** Transcript levels of the *GhPGF* gene in T_0 transgenic plants expressing the LwaCas13a, PbuCas13b, RfxCas13d, Cas13x.1, Cas13x.2, Cas13y.1, and Cas13y.2 systems, respectively. Error bars represent the mean ± S.D. ($n = 3$). Regenerated plants were assigned numerical identifiers based on the classification of Cas13 protein subfamilies and the target gene *GhPGF*. For instance, the label AP# indicates T_0 generation plants that underwent LwaCas13a-mediated knockdown of the *GhPGF* gene, while the corresponding T_1 generation is designated as AP#L. **h** Comparison of the knockdown efficiency of *GhPGF* transcripts mediated by various Cas13 orthologs in T_0 plants. **i** Phenotypes of T_0 transgenic plants expressing different Cas13 proteins. Bars, 5 cm. **j** Phenotypes of cotton bolls in T_0 transgenic plants. Bars, 1 cm

gossypol content in leaves from both edited and control plants. Analysis revealed a significant reduction in gossypol levels in the leaves of T_0 edited plants (Fig. 4b). As expected, the number of glands on cotton bolls and the gossypol content in the leaves were consistent with the downregulation trend of *GhPGF* transcripts.

More than 6 independent T_1 lines at the 6-week-old stage, which exhibited well-expressed Cas13 proteins, were selected for further evaluation of editing stability (Additional file 1: Fig. S5a-S5e). The transcript levels of *GhPGF* were consistently suppressed, demonstrating an average downregulation of 53.8% for LwaCas13a, 56.1% for PbuCas13b, 34.2% for RfxCas13d, 34.0% for Cas13x.1, 31.3% for Cas13x.2, 33.5% for Cas13y.1, and 34.7% for Cas13y.2 (Fig. 4c & d). This downregulation exhibited a similar trend with the editing efficiencies observed in T_0 plants (Fig. 4e). Meanwhile, several seeds from the T_1 generation were randomly selected and incubated until germination, revealing a significant reduction in gossypol glands compared to the control (Fig. 4f). Analysis of gossypol content in cotton bolls indicated a substantial decrease in T_1 plants at the same developmental stage, particularly among those edited with RfxCas13d, Cas13x, and Cas13y (Fig. 4g). In the presence of CRISPR/Cas13 proteins, both the knockdown effects and the resulting phenotypes can be stably inherited across subsequent generations. Notably, T_2 progeny lacking CRISPR/Cas13 proteins

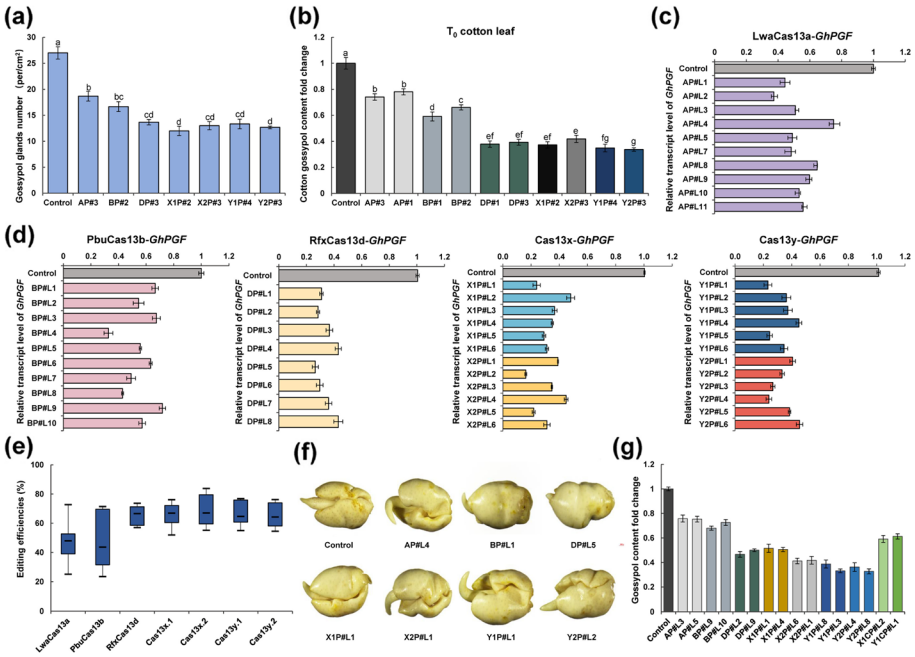

Fig. 4 Downregulation of *GhPGF* transcripts leads to a reduced gland phenotype in cotton. **a** Gland number of transgenic cotton bolls per cm^2. Statistical significance denoted by differing letters at $P < 0.05$ as determined by Student's t-test. **b** Gossypol content in the leaves of T_0 transgenic plants. Statistical significance denoted by differing letters at $P < 0.05$ as determined by Student's t-test. **c-d** Transcript levels of the *GhPGF* gene in T_1 transgenic plants expressing the LwaCas13a, PbuCas13b, RfxCas13d, Cas13x.1, Cas13x.2, Cas13y.1, and Cas13y.2 systems, respectively. **e** Comparison of the knockdown efficiency of *GhPGF* transcripts mediated by various Cas13 orthologs in T_1 plants. **f** Phenotypes of T_1 seeds observed under a stereomicroscope; Control: wild-type seeds; Bars, 1000 μm. **g** Relative gossypol content in T_1 cotton bolls. Error bars represent the mean ± S.D. ($n = 3$)

exhibited no significant differences in transcript levels of the targeted genes *GhCLA* and *GhPGF* compared to wild-type plants (Additional file 1: Fig. S5f).

In conclusion, all seven CRISPR/Cas13 orthologs, derived from five distinct subtypes, have been demonstrated to effectively utilize either a single crRNA or two crRNAs for the programmable knockdown of endogenous transcripts in plants. RfxCas13d, Cas13x.1, and Cas13x.2 exhibit enhanced stability and achieve editing efficiencies exceeding 58%, with a maximum efficiency recorded at 80%. Following these, Cas13y.1 and Cas13y.2 show editing efficiencies ranging from 50 to 78% and 43% to 76%, respectively. In contrast, LwaCas13a displays the lowest level of mRNA decay activity, while PbuCas13b shows slightly higher activity compared to LwaCas13a. No silencing effect on target genes was observed in T_2 progeny lacking CRISPR/Cas13 proteins after the segregation of T-DNA insertion events. It has been reported that Cas13 may exert toxic effects, potentially due to its RNase activity associated with pre-crRNA processing [54–57]. However, no significant toxic effects of Cas13 have been observed in cotton embryos or mature plants, which aligns with findings from other plant studies [27, 43].

Both Cas13x.1 and Cas13y.1 orthologs mediate the simultaneous knockdown of *GhCLA* and *GhPGF* transcripts

We integrated two guide crRNAs into a single vector to assess the capability of CRISPR/Cas13 for the simultaneous knockdown of two transcripts, aiming to extend

its application for multiplexed editing in plants. The Cas13x.1 and Cas13y.1 orthologs were selected to target the *GhCLA* and *GhPGF* genes, respectively. Therefore, crRNA-T (targeting *GhCLA*) and the crRNA-T1 (targeting *GhPGF*) were chosen to construct the vectors Cas13x.1-*GhCLA*-*GhPGF* and Cas13y.1-*GhCLA*-*GhPGF*, respectively (Fig. 5a). More than 8 transgenic plants were generated through *Agrobacterium*-mediated transformation (Additional file 2: Table S4), in which either Cas13x.1 or Cas13y.1 protein was successfully expressed (Additional file 1: Fig. S5g & S5h). The designations X1CP# and Y1CP# refer to T_0 generation plants that underwent the knockdown of both the *GhCLA* and *GhPGF* genes, mediated by either the Cas13x.1 or Cas13y.1 systems. The corresponding T_1 generation plants are designated as X1CP#L and Y1CP#L.

The transcript levels of *GhCLA* and *GhPGF* were significantly reduced to 31.2% and 26.7%, respectively, in the X1CP#8 plant. In the Cas13x.1-*GhCLA*-*GhPGF* edited plants, the average transcription abundance of *GhCLA* and *GhPGF* transcripts decreased to 38.5% and 50%, respectively (Fig. 5b). For the Cas13y.1-*GhCLA*-*GhPGF* edited plants, transcript levels of *GhCLA* and *GhPGF* were notably diminished to 28.4% and 30% in Y1CP#2; additionally, their average transcription abundances decreased to 30.6% and

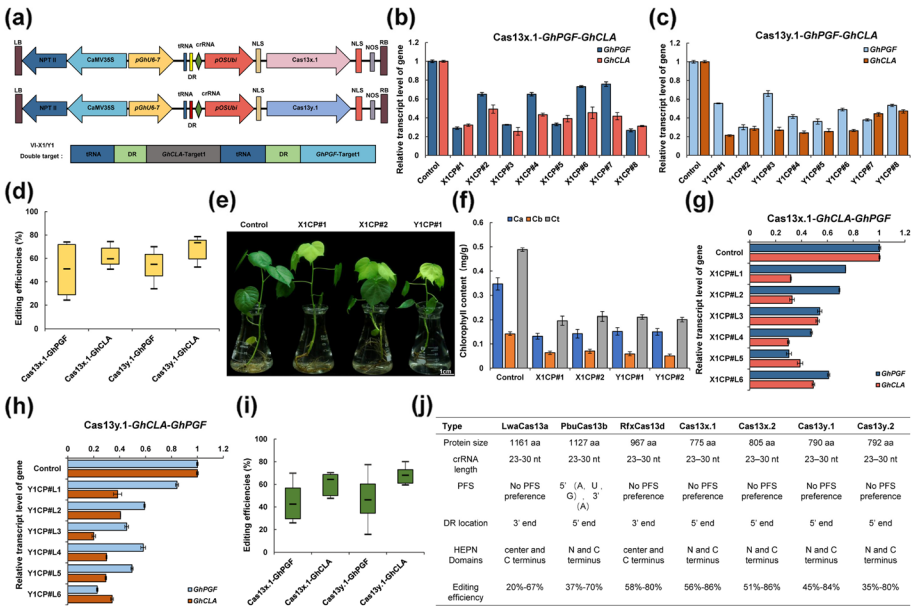

Type	LwaCas13a	PbuCas13b	RfxCas13d	Cas13x.1	Cas13x.2	Cas13y.1	Cas13y.2
Protein size	1161 aa	1127 aa	967 aa	775 aa	805 aa	790 aa	792 aa
crRNA length	23-30 nt	23-30 nt	23–30 nt	23–30 nt	23–30 nt	23–30 nt	23–30 nt
PFS	No PFS preference	5′ (A, U, G) ; 3′ (A)	No PFS preference	No PFS preference	No PFS preference	No PFS preference	No PFS preference
DR location	3′ end	5′ end	3′ end	5′ end	5′ end	5′ end	5′ end
HEPN Domains	center and C terminus	N and C terminus	center and C terminus	N and C terminus	N and C terminus	N and C terminus	N and C terminus
Editing efficiency	20%-67%	37%-70%	58%-80%	56%-86%	51%-86%	45%-84%	35%-80%

Fig. 5 Cas13x.1 and Cas13y.1 effectively mediate the simultaneous knockdown of *GhCLA* and *GhPGF* transcripts. **a** Schematic representation of a multi-guide expression cassette designed to simultaneously target the endogenous transcripts *GhCLA* and *GhPGF*. **b** Transcript levels of the *GhPGF* and *GhCLA* genes in T_0 transgenic plants expressing the Cas13x.1 system. **c** Transcript levels of the *GhPGF* and *GhCLA* genes in T_0 transgenic plants expressing the Cas13y.1 system. **b-c** Error bars represent the mean ± S.D. ($n = 3$). The designations X1CP# and Y1CP# refer to T_0 generation plants that underwent knockdown of both the *GhCLA* and *GhPGF* genes, mediated by either the Cas13x.1 or Cas13y.1 systems. The corresponding T_1 generation plants are designated as X1CP#L and Y1CP#L. **d** Comparison of the knockdown efficiency of *GhCLA* and *GhPGF* transcripts mediated by the Cas13x.1 and Cas13y.1 systems in T_0 regenerated plants. **e** Chlorophyll fading phenotypes of T_0 transgenic plants edited with Cas13x.1 and Cas13y.1. Bars, 1 cm. **f** Chlorophyll content in the leaves of T_0 plants expressing the Cas13x.1 and Cas13y.1 systems. Error bars represent the mean ± S.D. ($n = 3$). **g** Transcript levels of target genes in T_1 transgenic plants mediated by the Cas13x.1 system. **h** Transcript levels of target genes in T_1 transgenic plants mediated by the Cas13y.1 system. **i** Comparison of the knockdown efficiency of *GhCLA* and *GhPGF* transcripts mediated by the Cas13x.1 and Cas13y.1 systems in T_1 plants. Error bars represent the mean ± S.D. ($n = 3$). **j** Characteristics and editing efficiencies of the seven Cas13 orthologs

46.2%, respectively (Fig. 5c). As anticipated, Cas13x.1 and Cas13y.1 can simultaneously degrade two endogenous transcripts, resulting in a reduction in RNA abundance for both the *GhCLA* and *GhPGF* genes, with an average editing efficiency of up to 50% (Fig. 5d). These edited plants displayed a chlorophyll-fading phenotype (Fig. 5e), with chlorophyll content declining to 40.1% in X1CP#1 and 43.6% in X1CP#2, respectively. Similarly, chlorophyll content was reduced to 43.1% in Y1CP#1 and 41.1% in Y1CP#2 compared to control plants (Fig. 5f).

Six positive T_1 lines for each vector were identified and selected for the analysis of RNA transcription abundance (Additional file 1: Fig. S5i). Furthermore, several seeds from T_1 generation were randomly chosen and incubated until germination. The number of gossypol glands in the germinated T_1 seeds showed a significant reduction compared to the control (Additional file 1: Fig. S6a). The average transcript levels of the *GhCLA* and *GhPGF* genes decreased by 60.8% and 44% for Cas13x.1 (Fig. 5g), and by 68% and 46.8% for Cas13y.1, respectively (Fig. 5h). Both Cas13x.1 and Cas13y.1 efficiently mediated multiple RNA knockdown events, achieving higher efficiency than traditional technologies (Fig. 5i). These findings provide the first evidence that CRISPR/Cas13 systems enable precise editing of multiple transcripts in plants, resulting in phenotypic traits with stable heritability. Consequently, a summary table was created to elucidate the editing characteristics associated with various Cas13 orthologs, encompassing aspects such as protein size, structural features, preferences for PAM sequences, positions of DR sequences, and editing efficiency (Fig. 5j).

Efficient RNA interference targeting of TRV transcripts in tobacco plants

Subsequently, we conducted a comprehensive evaluation of the interference activities exhibited by these CRISPR/Cas13 systems in targeting exogenous RNA viruses. TMV (*Tobacco mosaic virus*), one of the most destructive single-stranded RNA viruses affecting over 200 plant species, was chosen as the target virus. An analysis of the TMV genome revealed four open reading frames (ORF) that encode two replicative enzymes. Two crRNAs (crRNA1 and crRNA2) were designed to target conserved regions within TMV (Fig. 6a). TRV (*Tobacco rattle virus*) was selected as an additional target, and crRNA3 was designed to target the CP region of TRV RNA2 (Fig. 6b). *Agrobacterium*-mediated transformation was employed to generate stable transgenic plants of *N. benthamiana* plants expressing various Cas13 orthologs, including LwaCas13a-TMV (A-TMV), PbuCas13b-TMV (B-TMV), RfxCas13d-TMV (D-TMV), Cas13x.1-TMV (X1-TMV), Cas13x.2-TMV (X2-TMV), Cas13y.1-TMV (Y1-TMV), Cas13y.2-TMV (Y2-TMV), LwaCas13a-TRV (A-TRV), and PbuCas13b-TRV (B-TRV) (Fig. 6c & Additional file 2: Table S5). Regenerated plants were assigned numerical identifiers based on the designation of Cas13 protein subfamilies and their corresponding target viruses. For example, T_0 generation plants are designated as A-TMV#, while the corresponding T_1 generation plants are labeled as A-TMV#L. Notably, no abnormalities in growth or development were observed throughout the regenerative transformation process.

An optimized TRV-RNA-based fluorescent reporter system expressing the *GFP* gene effectively monitors the dissemination of the CP-GFP fusion protein in tobacco leaves, thereby facilitating visualization of the viral infection process (Fig. 6d). More than 9 independent transgenic plants of A-TRV and B-TRV were selected for TRV infection,

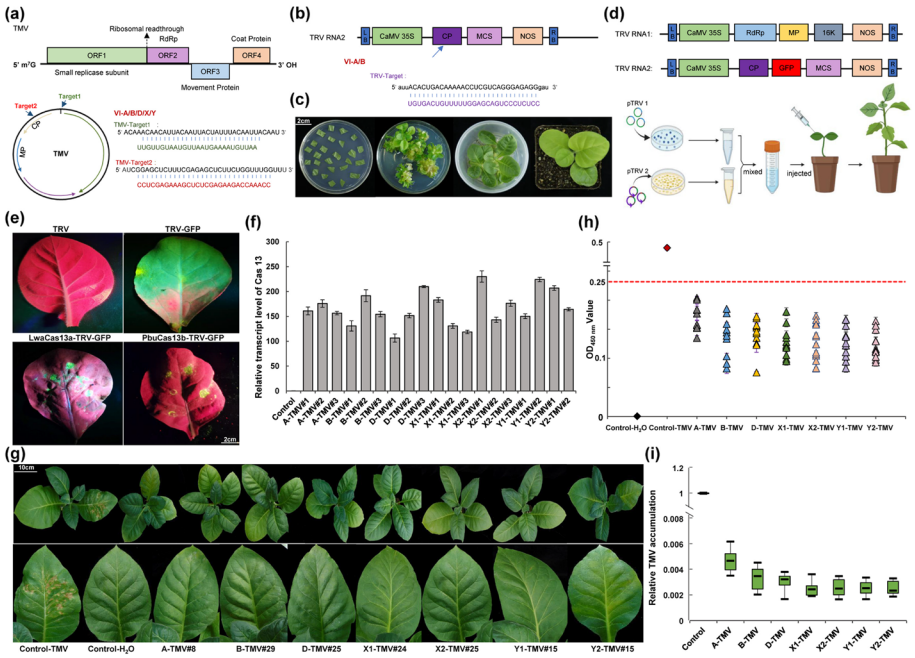

Fig. 6 Various Cas13 orthologs for RNA interference in tobacco plants. **a** Schematic representation of TMV and detailed information on the targeted sequences for various Cas13 orthologs. **b** Structure of TRV RNA2 along with specific details of the crRNA sequences. **c** *Agrobacterium*-mediated genetic transformation of tobacco, utilizing the K326 as the transformation recipient. Bars, 2 cm. **d** The TRV system expressing GFP was employed as a reporter system to evaluate Cas13 activity in transient assays. GFP: green fluorescent protein. **e** Monitoring GFP expression to assess Cas13-mediated viral interference activities in tobacco leaves during transient assays. Bars, 2 cm. **f** Relative transcript levels of different *Cas13* genes in T_0 transgenic tobacco plants. Regenerated plants were assigned numerical identifiers based on the classification of Cas13 protein subfamilies and their target viruses. For instance, T_0 generation plants are designated as A-TMV#, while the corresponding T_1 generation plants are labeled as A-TMV#L. **g** Disease symptoms observed in T_0 transgenic plants infected with TMV at 7 dpi. Bars, 10 cm. **h** Virus accumulation assessed at 7 dpi using ELISA. **i** Virus accumulation evaluated at 7 dpi through qRT-PCR. Error bars represent the mean ± S.D. ($n = 3$)

exhibiting relatively comparable levels of Cas13 protein expression (Additional file 1: Fig. S6b & S6c). Consistent with our previous findings, both Cas13 orthologs exhibited RNA interference activity against TRV. Notably, a reduction in GFP fluorescence was observed in the edited TRV-GFP leaves, with PbuCas13b demonstrating greater interference activity compared to LwaCas13a (Fig. 6e). This finding underscores the functionality and efficacy of the CRISPR/Cas13 system in mediating viral interference *in planta*.

Different Cas13 orthologs confer efficient interference against TMV infection

Randomly selected positive T_0 transgenic plants (15 individuals per Cas13 system) were inoculated with TMV at the 3-week-old stage, and their viral resistance was subsequently assessed through symptom evaluation and molecular analysis (Fig. 6f). Wild-type tobacco plants were inoculated with TMV as positive controls, while those treated with H_2O served as negative controls. We observed that TMV-infected wild-type plants exhibited typical viral symptoms at 7 days post-inoculation (dpi), including a mosaic pattern, pronounced leaf shrinkage, and curling. In contrast, T_0 transgenic plants displayed no symptoms and maintained normal developmental morphology, closely resembling that of H_2O-treated wild-type plants (Fig. 6g).

Serological analysis using enzyme-linked immunosorbent assays (ELISA) was performed on the selected plants. Compared to positive controls, viral titers in most transgenic plants were below detection limits (less than 0.25), indicating that the majority of tested transgenic plants exhibit resistance to TMV infection. The number of resistant plants identified by ELISA included 9 (60.0%) for A-TMV, 10 (66.7%) for B-TMV, 12 (80.0%) for D-TMV, 13 (86.7%) for X1-TMV, 13 (86.7%) for X2-TMV, 13 (86.7%) for Y1-TMV, and 13 (86.7%) for Y2-TMV (Fig. 6h). The resistance of transgenic plants to TMV was further validated through qRT-PCR assays, which revealed a significant reduction in TMV transcript accumulation in leaves at 7 dpi (Fig. 6i). These findings suggest that Cas13 systems can effectively facilitate the degradation of specific viral RNA sequences, thereby conferring resistance to TMV in transgenic plants.

Stable inheritance of resistance to TMV in transgenic tobacco progeny

Positive T_1 transgenic plants (10 individuals per Cas13 system) were subsequently infected with TMV to further assess their resistance at the 3-week-old stage. Wild-type plants exhibited typical mosaic leaf symptoms beginning at 7 dpi. By 40 dpi, the entire plant displayed noticeable growth deformities and dwarfism, resulting in a marked reduction in seed yield. In contrast, most transgenic lines showed only mild symptoms; notably, some transgenic plants edited with RfxCas13d, Cas13x, and Cas13y showed no apparent symptoms at 40 dpi (Fig. 7a). The markedly reduced accumulation of TMV in the leaves of transgenic plants at 40 dpi was further corroborated by ELISA and qRT-PCR assays (Fig. 7b & c). Similar results were observed in the T_0 generation, suggesting that TMV resistance mediated by the CRISPR/Cas13 system is heritable.

Transgenic lines exhibiting varying expression levels of Cas13/crRNA, with differences ranging from 2- to 3-fold, were selected to assess their resistance to TMV (Fig. 7d & Additional file 1: Fig. S6d). Severe mosaic symptoms were observed in TMV-infected wild-type plants; however, transgenic lines with low expression levels (e.g., A-TMV#L6) displayed mild mosaic symptoms (Additional file 1: Fig. S6e). In contrast, the transgenic lines with high expression levels (e.g., A-TMV#L2) showed no obvious symptoms. The positive correlation between Cas13/crRNA expression and the inhibition of TMV accumulation is further substantiated by the aforementioned ELISA and qRT-PCR data.

To investigate the detrimental effects after TMV infection, we further assessed the levels of reactive oxygen species (ROS), hydrogen peroxide (H_2O_2), and superoxide dismutase (SOD) in TMV-inoculated transgenic plants expressing various Cas13 orthologs at 7 dpi. Similarly, wild-type tobacco plants were inoculated with TMV as positive controls, while those treated with H_2O served as negative controls. A higher accumulation of ROS and H_2O_2 was observed in TMV-infected wild-type plants, whereas transgenic plants exhibited significantly lower levels of these compounds in the infected leaves. Notably, minimal to no accumulation of ROS and H_2O_2 was detected in the leaves of wild-type plants treated with H_2O (Fig. 7e & f). Meanwhile, the antioxidant activity of SOD was significantly elevated, peaking in wild-type plants infected with TMV, and exceeding the levels observed in transgenic plants (Fig. 7g). Collectively, these findings indicate that resistant transgenic plants exhibit minimal damage due to the effective expression of Cas13/crRNA, which facilitates the degradation of TMV transcripts and reduces the accumulation of TMV particles.

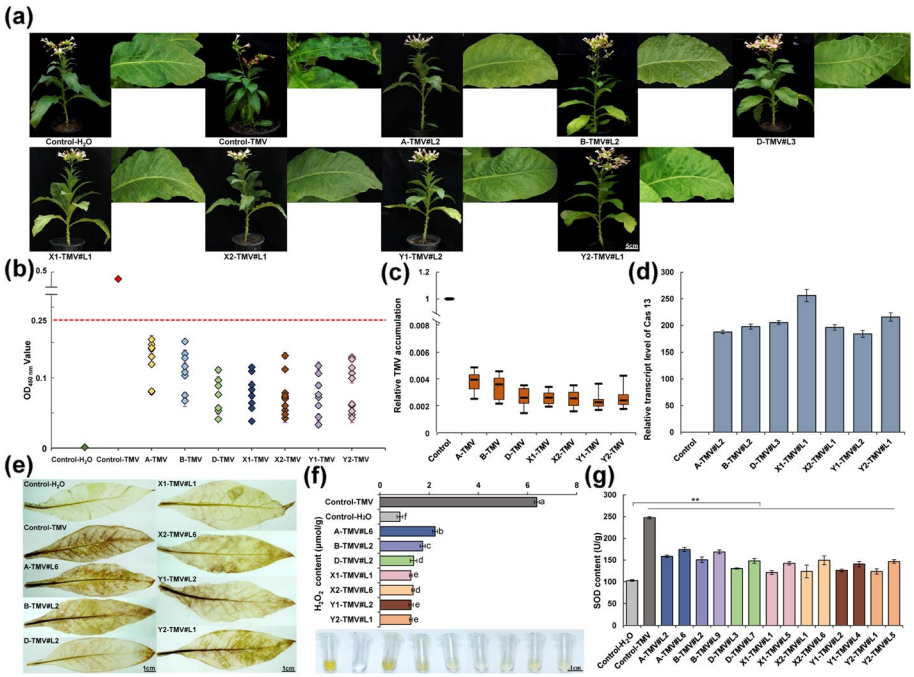

Fig. 7 Stable inheritance of resistance to TMV in transgenic tobacco progeny. **a** Symptoms observed in T_1 transgenic and wild-type plants infected with TMV at 40 dpi. Bars, 5 cm. **b** Virus accumulation was assessed at 7 dpi using ELISA in T_1 transgenic plants. **c** Virus accumulation was quantified at 7 dpi using qRT-PCR. **d** Transcript levels of various *Cas13* genes in T_1 transgenic tobacco plants. **e** DAB staining was performed on infiltrated leaves of transgenic and control plants at 7 dpi. Bars, 1 cm. **f** H_2O_2 content was measured in leaves from different transgenic and wild-type plants at 7 dpi, with representative wells containing H_2O_2 extract shown below (in yellow). Statistical significance is denoted by differing letters at $P < 0.05$ using Student's t-test. **g** SOD activity was measured in the leaves of various transgenic and wild-type plants at 7 dpi. Error bars represent the mean ± S.D. ($n = 3$). $^{**}P < 0.01$

Limited off-target effects were revealed in different Cas13 transgenic cotton plants

We further examined the specificity of Cas13 systems for transcript knockdown by assessing potential off-target effects. First, we analyzed the designed crRNAs targeting *GhCLA* and *GhPGF* transcripts for sequence similarity with other sequences using whole-transcriptome BLAST. Our findings indicated that the crRNA targeting *GhCLA* exhibited at least 7-nt mismatches with non-target sequences (Additional file 2: Table S6), whereas the crRNAs directed against *GhPGF* displayed a minimum of 5-nt mismatches with other non-target sequences (Additional file 2: Table S7). Subsequently, we performed transcriptome profiling through RNA sequencing (RNA-seq) on transgenic plants expressing various Cas13 orthologs (Additional file 1: Fig. S6f & S6g).

A comparative analysis was conducted on T_1 generation plants expressing the LwaCas13a, PbuCas13b, RfxCas13d, Cas13x.1, Cas13x.2, Cas13y.1, and Cas13y.2 systems to edit the *GhCLA* gene. We did not observe any global downregulation of mRNA that could arise from the collateral activity of Cas13. Compared to the control group, hundreds of genes were significantly altered (|fold change| > 1.5; Padj < 0.05), with a notably higher number of upregulated genes than downregulated ones across individual samples (Fig. 8a). Each Cas13 ortholog influenced the RNA expression of some ortholog-specific genes; however, some consistency was observed among the

various Cas13 samples simultaneously (Fig. 8b). All predicted off-target transcripts were found to be insignificantly regulated by these Cas13 systems.

We further examined specific sets of differentially expressed genes (DEGs) associated with each ortholog to identify their enriched functional terms. The analysis of KEGG pathway enrichment revealed that downregulated DEGs were predominantly linked to pathways related to riboflavin metabolism, phenylpropanoid biosynthesis and tryptophan metabolism (Fig. 8c). Despite both Cas13-associated and Cas13-regulated RNAs were enriched for several genes, we did not observe significant correlation between Cas13 binding and Cas13-induced gene expression change (Additional file 1: Fig. S6h). These findings provide compelling evidence that the identified downregulated DEGs are not attributable to conventional off-target effects. The enriched functional pathways associated with these DEGs are primarily related to plant growth and development, complicating the assessment of whether these differences arise from the collateral activity of the Cas13 protein or from background noise.

Furthermore, we performed RNA-seq analysis on T_1 generation plants expressing the Cas13x.2 system, which specifically targets and degrades the transcripts of *GhCLA* (designated as Cas13X2C) and *GhPGF* (designated as Cas13X2P). Our results indicated that Cas13x.2 induced a substantial number of DEGs following the knockdown of either *GhCLA* or *GhPGF* (Fig. 8d & Additional file 1: Fig. S6i). We further compared the downregulated DEGs and identified their enriched functional terms. Among the top 30

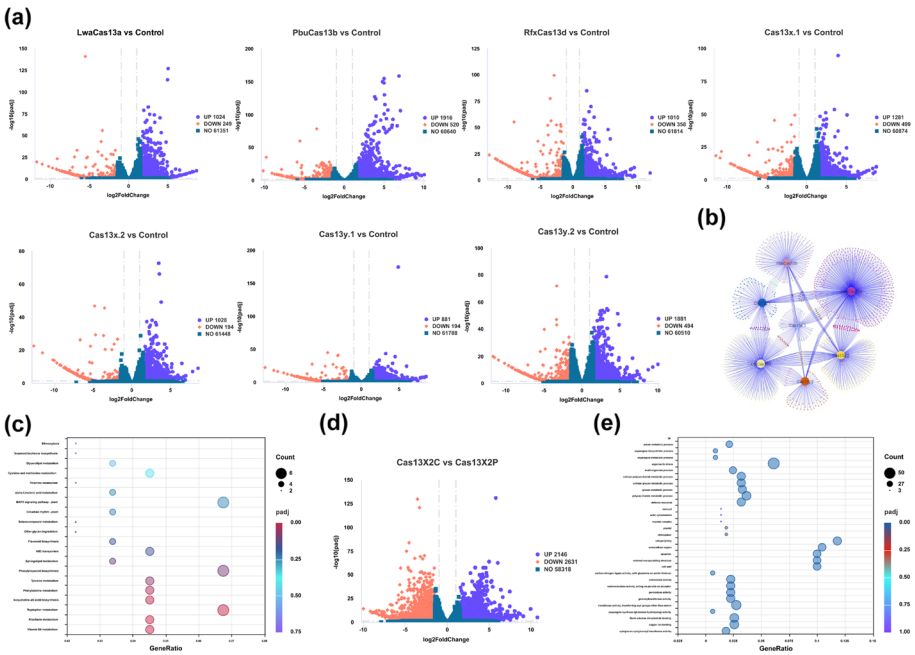

Fig. 8 Off-target analysis of various Cas13 orthologs. **a** Volcano plots illustrating the down- and up-regulated DEGs for various Cas13 orthologs, including LwaCas13a, PbuCas13b, RfxCas13d, Cas13x.1, Cas13x.2, Cas13y.1, and Cas13y.2, in comparison to the control, which mediates the knockdown of the *GhCLA* gene. **b** Overlap of DEGs among transgenic plants across various Cas13 orthologs. **c** The top 20 KEGG pathways enriched with downregulated DEGs among seven Cas13 orthologs. **d** Volcano plots of down- and up-regulated DEGs, Cas13X2C versus Cas13X2P. **e** Process-related Gene Ontology (GO) categories enriched in genes regulated by various Cas13 orthologs targeting *GhCLA* and G*hPGF*, respectively. RNA-seq analysis was performed using three independent biological replicates

downregulated functional categories, 5 were found to be regulated by *GhCLA* and 3 categories were regulated by *GhPGF* (Fig. 8e). KEGG pathway enrichment analysis revealed that the downregulated DEGs were mainly enriched in pathways related to phenylpropanoid biosynthesis, ABC transporters, and plant-pathogen interaction (Additional file 1: Fig. S6j). These findings suggest that the production of certain downregulated DEGs may arise from the knockdown of target transcripts or in response to external defense mechanisms. The limited number of remaining DEGs, which is nearly negligible in comparison to the extensive cotton genome, may be attributed to background noise. Overall, CRISPR/Cas13 serves as a precise and reliable tool for RNA knockdown, exhibiting high efficiency and minimal off-target effects.

Discussion

CRISPR/Cas9 system has emerged as a remarkable tool for the precise manipulation of DNA in plants [58–60]. It has been widely used for genetic modifications, disease diagnostics, and crop improvement across various organisms [61–63]. In contrast, the CRISPR/Cas13 system serves as a robust mechanism for RNA degradation, allowing for highly efficient and precise alterations without modifying the underlying DNA sequence. Its compact structure, combined with inherent multiplexing capabilities, significantly enhances its applicability in fundamental research within RNA biology as well as in RNA-based diagnostic and therapeutic applications. Moreover, the continuously expanding dead Cas13 (dCas13) toolkit facilitates a diverse array of RNA manipulations with single-nucleotide precision and specificity [64–68]. Currently, various subtypes of Cas13 proteins exhibit differences in size, off-target effects, collateral activity, toxicity, and efficacy in eukaryotic cells. However, a significant number of active Cas13 proteins remain uncharacterized in plant systems, primarily due to the complexities inherent in plant genomes and the challenges associated with genetic transformation. Notably, the application of Cas13 for the knockdown of endogenous mRNA has been explored in a limited number of studies, the majority of which focus on the Cas13a subtype. In this study, we investigated seven Cas13 orthologs from five subtypes: LwaCas13a (VI-A), PbuCas13b (VI-B), RfxCas13d (VI-D), Cas13x.1 (VI-X), Cas13x.2 (VI-X), Cas13y.1 (VI-Y), and Cas13y.2 (VI-Y). A comprehensive evaluation of various CRISPR/Cas13 nucleases was conducted to achieve effective transcriptome editing of both endogenous transcripts and RNA viruses, enabling us to identify the most catalytically active Cas13 orthologs that are suitable for plant transcriptome editing.

Through a systematic assessment of multiple CRISPR/Cas13 nucleases, we identified seven CRISPR/Cas13 systems that are capable of cleaving targeted mRNA and reducing the levels of specific transcripts. RfxCas13d, Cas13x, and Cas13y demonstrated higher editing efficiency when using the same crRNA, followed by PbuCas13b, and then LwaCas13a. Our findings indicate that Cas13 orthologs, particularly LwaCas13a and PbuCas13b, exhibit significantly lower editing efficiency in plant systems compared to the levels observed in mammalian cells. The observed discrepancy may be attributed to several factors, including the expression levels of Cas13/crRNA, the specific insertion sites of T-DNA, and the types of cells involved. Notably, the editing efficiency of Cas13

systems for the simultaneous degradation of two endogenous transcripts is evaluated for the first time in plants, providing evidence for the potential utility of employing Cas13 orthologs in multiplexed editing. The transient expression of the TRV-GFP fluorescent reporter system visually demonstrated that the Cas13 systems effectively degraded the target TRV transcripts, thereby inhibiting viral transmission. Viral inoculation assays revealed that the successfully expressed Cas13/crRNA effectively cleaved or degraded TMV transcripts, resulting in a reduced accumulation of viral particles.

Despite the capabilities of CRISPR/Cas13 to target ssRNA across various organisms, inherent limitations associated with RNA targeting and binding that may constrain its applications. A significant limitation is the collateral activity of Cas13, which can lead to nonspecific RNA cleavage [18, 45, 69]. It has been reported that the collateral activity of Cas13 may result in chromatin collapse, potentially contributing to global mRNA downregulation and inhibition of DNA replication [16, 70]. However, we did not observe any global downregulation of mRNA that could arise from the collateral activity of Cas13. Moreover, the transgenic plants exhibited no significant growth defects or variations. RNA-seq analysis of various samples identified several downregulated DEGs in our study, with some DEGs are associated with target transcripts and others are linked to external defense responses. The limited number of remaining DEGs, which is nearly negligible compared to the extensive cotton genome, complicates the assessment of whether these DEGs can be attributed to background noise or represent a side effect of the paracrine activity of Cas13. Importantly, all predicted off-target transcripts were found to be not significantly regulated by these Cas13 systems. These findings indicate that CRISPR/Cas13 functions as a precise and reliable tool for RNA knockdown, exhibiting minimal off-target effects. While substantial and unequivocal evidence supports the existence of collateral activity for Cas13 in vitro and within bacterial systems, the extent of this activity appears to vary across different studies conducted on eukaryotic cells. Recent investigations indicate that the extent of collateral activity is significantly influenced by multiple factors, including cell type [18, 70], target RNA abundance [17, 44, 70], subtypes of Cas13 proteins [17], expression levels of Cas13/crRNA [7], and even cellular pH [71–73]. These factors may elucidate the contradictory results reported in the literature.

Previous studies have reported neurotoxic and embryotoxic effects associated with certain Cas13 enzymes in mammalian cells [54, 56]. However, callus and transgenic plants containing seven Cas13 systems (in cotton and tobacco) did not show any significant toxic effect during the genetic transformation process in our study. Transcriptome analyses further indicated limited differences in the downregulation of gene expression among the seven Cas13 proteins. Additional research is warranted to explore alternative strategies aimed at mitigating the toxic effects and collateral activity of Cas13 in various organisms. A few studies on insects and plants have reported that, in the absence of Cas13, crRNA alone can effectively knockdown target RNAs, thereby facilitating RNA interference [74]. Our findings demonstrate that the CRISPR/Cas13 enables the stable inheritance of gene knockdown effects and associated phenotypes across generations. The transgenic progeny that exhibited trait segregation, resulting in plants devoid

of CRISPR/Cas13 proteins, did not show significant differences in the transcript levels of target genes when compared to wild-type plants. Individual controls for crRNA and Cas13 are crucial for accurately evaluating such activity. Therefore, further investigation is warranted to ascertain whether this phenomenon can occur in the presence of both Cas13 and crRNA.

Conclusions

In summary, the CRISPR/Cas13 approach offers a robust and reliable platform for transcriptome editing in gene analysis and plant research, with considerable potential for applications in transcriptome engineering.

Methods

Vector construction

Seven Cas13 orthologs were codon-optimized and synthesized by Kingsley Company. The pRGEB32-GhU6.7-NPTII vector was linearized using *Bst*BI and *Xba*I. Subsequently, the full-length Cas13 was ligated into the linearized pRGEB32-GhU6.7-NPTII using the ClonExpress® II One Step Cloning Kit to obtain pRGEB32-GhU6.7-Cas13-NPTII. The tRNA-gRNA transcription unit has been used to effectively enhance crRNA transcription in the CRISPR/Cas system for plant genome editing [47, 75, 76]. In this study, the p*GhU6-7* was selected to drive the crRNAs transcription. The sequences of these Cas13 orthologs are provided in Additional file 3.

Vector construction of the TRV-GFP system

By comparing the original sequence of TRV RNA2 with the actual sequence of the sequenced TRV vector, we identified the location of the viral coat protein of the TRV2 vector. Using *Gateway* cloning, we ligated the amplified GFP sequence into the *pGWB404* vector. The TRV CP-encoding sequence has been fused with the GFP-encoding sequence, thereby preserving its capacity for efficient replication and expression of the GFP protein in infected leaves.

Construction of crRNAs targeting different transcripts

The crRNAs targeting specific transcripts were designed using Cas13 design (https://cas13design.nygenome.org/) and subsequently verified using the NCBI BLAST (https://blast.ncbi.nlm.nih.gov/Blast.cgi) to minimize unwanted mRNA off-target bindings in the cotton genome. The sequences of TMV and TRV were retrieved from NCBI Reference Sequence: NC_001367.1 and NC_003811.1, while the sequences of the *GhCLA* and *GhPGF* genes were obtained from Cotton FGD (https://cottonfgd.net/). All the corresponding crRNAs sequences are listed in Additional file 1: Table S1.

Genetic transformation

The vectors constructed for the target genes were introduced into *Agrobacterium* strain GV3101 via electroporation. The upland cotton (*Gossypium hirsutum L.*) cultivar JIN668 served as the recipient for transformation [77]. Seeds were sterilized and cultured in a

dark chamber for 5–6 days at 30 °C. Hypocotyls were excised into 5–7 mm segments and used as explants for *Agrobacterium*-mediated transformation, following our previous reports [78]. *Nicotiana benthamiana* (K326) was used as the recipient for transformation using the leaf disk method. Seedlings were subsequently transferred to a nutrient solution for hydroponic cultivation for an additional 3–5 days prior to being planted in the greenhouse.

Molecular analyses of transgenic plants

Genomic DNA was extracted using the CTAB method, and positive transformants were identified by PCR with corresponding Cas13-specific primers. Total RNA was extracted and reverse-transcribed into cDNA utilizing the Polysaccharide Polyphenol RNA Extraction Kit (Tiangen, China). For each sample, 3 μg of total RNA was transcribed into cDNA using M-MLV reverse transcriptase (Promega, USA). Real-time PCR was conducted on a CFX96 real-time PCR system employing SYBR Green Supermax (Bio-Rad Laboratories, CA, USA). The thermal cycling parameters were as follows: 95 °C for 2 min, followed by 40 cycles of 95 °C for 15 s and 60 °C for 35 s. Empty vector-transformed plants (vector without crRNA) served as negative controls. qRT-PCR results were analyzed using the $2^{-\Delta\Delta CT}$ method, where differences between average CT values of target genes and the reference gene *GhUBQ7* from three biological replicates were used to calculate the relative expression levels of target genes, normalized against control groups. All primers are listed in Additional file 2: Table S8.

RNA-seq and analysis

To analyze the functional specificity of Cas13 effectors, RNA was extracted with above method, fragmented and reverse-transcribed to cDNA with a *HiScript* II One Step RT-PCR Kit according to the manufacturer protocol. An RNA-seq library was generated with a TruSeq Stranded Total RNA library preparation kit using the standard protocol. The transcriptome libraries were sequenced using a 150-bp paired-end Illumina Xten platform. RNA-seq data were analyzed as previously described and presented as the mean of all repeats [79]. DESeq2 (ref. 47) was used to calculate differentially expressed genes. Genes with $|\text{fold change}| > 1.5$, adjusted $P < 0.05$ were treated as differentially expressed genes. A customized script, HTSeq2FPKM.pl, was used to calculate fragments per kilobase per million mapped fragments (FPKM) values from the read count matrix for plotting visualization. RNA-seq analysis was performed with three independent biological replicates.

TRV inoculation

The pTRV1 and pTRV2 strains were activated in 10 mL of LB medium at 28 °C with shaking at 200 rpm for a duration of 16 h. Subsequently, the broth was collected into a 10 mL centrifuge tube and subjected to centrifugation at 4000 rpm for 15 min. The resuspension solution containing pTRV1 and pTRV2 was mixed in equal volumes (1:1), maintaining optical densities (OD_{600}) between 0.6 and 1.2. *Agrobacterium* strains carrying the binary pTRV1, and the engineered pTRV2 genome harboring crRNAs against TRV-GFP genome were combined. In addition, the TMV-GFP infectious clones were

co-delivered into *N. benthamiana* leaves via *Agrobacterium* -infection. A non-specific crRNA (ns-crRNA) with no sequence similarity to the TMV-GFP genome served as a control. After 2 days of dark treatment, the GFP signals in the leaves of the infected plants were observed under ultraviolet (UV) light.

Detection of chlorophyll contents

Chlorophyll content was measured according to a previously established method with some modifications [80]. Absorbance was recorded at 663.6 nm and 646.6 nm using a spectrophotometer (UV757CRT, Shanghai). For chlorophyll extraction, the plant material was cut into 1 mm pieces and transferred to a 10 mL graduated test tube. Subsequently, 2 mL of dimethyl sulfoxide (DMSO) was added, and the tubes were incubated at 65 °C in the absence of light until the plant material became white or transparent. To dilute the DMSO extract, 8 mL of 80% (v/v) acetone was added, and absorbance was determined at both wavelengths using the spectrophotometer. Chlorophyll concentrations were calculated using the following formulas: Ca (mg L^{-1}) = $12.27 \times A_{663.6} - 2.52 \times A_{646.6}$; Cb (mg L^{-1}) = $20.10 \times A_{646.6} - 4.92 \times A_{663.6}$; Ct (mg L^{-1}) = Ca + Cb = $7.35 \times A_{663.6} + 17.58 \times A_{646.6}$. Three replicates were assayed for each sample.

Detection of gossypol content

Gossypol content was measured according to the aniline colorimetric method with some modifications [81]. A total of 5 g of the crushed sample was combined with 20 mL of glass beads (6 mm) and 3 mL of ascorbic acid solution, and then mixed by shaking for 3 min. The mixture was subsequently subjected to ultrasonic extraction and filtration. The filtrate was diluted to a final volume of 50 mL with the extraction reagent, and 4/5 mL portions of each filtrate were transferred to 25 mL test tubes, labeled as a, b, a_0, and b_0. Next, 0.5 mL of freshly evaporated aniline was added to tubes b and b_0, which were then heated at 75 °C for 40 min. After cooling, the solution was mixed with tubes a and b, and diluted to a final volume of 25 mL. The absorbance was measured at 445 nm using a spectrophotometer (UV757CRT, Shanghai). The absorbance A_0 of the blank assay solution b_0 was determined using a_0 as a reference, while the absorbance A of the sample assay solution b was determined using a as a reference. Therefore, the difference $A - A_0$ represented the absorbance value of the sample solution. Three replicates were conducted for each sample.

Tobacco cultivation and virus inoculation

Tobacco seeds were germinated at 25 ± 0.5 °C for 2–3 days and then evenly sown in a porcelain plate (30 cm in length, 20 cm in width, and 3 cm in height) filled with soil. Subsequently, the tobacco seedlings were cultivated in a GXZ-type light incubator maintained at 25 ± 0.5 °C, with a relative humidity of 75% ± 5%, under a photoperiod of 14 h of light and 10 h of darkness. At the eight to ten leaf stage, the tobacco plants were inoculated with TMV using the friction inoculation method.

Healthy transgenic tobacco plants were selected, and two control groups were established: a blank control group (wild-type plants + H_2O), which served as the negative

control, and an inoculation control group (wild-type plants + TMV), which served as the positive control. Three plants were randomly selected for each treatment, with three replicates conducted. Infected leaves were collected at 7 dpi and stored at -80 °C after being flash-frozen in liquid nitrogen to assess the activities of relevant defense enzymes.

Inoculation of TMV

Diseased leaves infected with TMV were collected for inoculation. The infected leaves were placed in a mortar, and a 0.01 M phosphate buffer solution (PBS, pH 7.2) was added at a dilution ratio of 1:6, followed by thorough grinding of the mixture. Subsequently, a small amount of diatomaceous earth was introduced, and the resulting mixture was gently applied to the leaf surfaces of both transgenic and control tobacco plants by wiping it 2–3 times with a finger dipped in the diseased leaf extract. It is crucial to ensure that the friction is gentle and unidirectional, moving from the base to the tip of each leaf. After 20 min post-inoculation, any residual disease sap and rubbing agent on the leaf surface should be rinsed off using a wash bottle. Two to three leaves from each plant were inoculated from top to bottom.

ELISA

Leaf samples collected independently from the plants were utilized for testing, and kits containing anti-TMV antibodies (Shanghai Huabang Biotech Co., China) were employed according to the manufacturer's protocols. Reactions were analyzed in triplicate, with the raw readings from the samples—optical density values at a wavelength of 450 nm—averaged and expressed as multiples of those obtained from negative controls. The criteria for test validity included: average optical density of positive control wells ≥ 1.00 and average optical density of negative control wells ≤ 0.15. The critical cutoff was calculated as follows: Critical = average optical density of negative control wells + 0.15. A sample was considered negative if its optical density was less than the critical cutoff, while a sample with an optical density equal to or greater than this value was deemed positive. Three replicates were conducted for each sample.

Staining and detection of H_2O_2

3,3'-diaminobenzidine (DAB) staining was employed to tfor the qualitative detection of hydrogen peroxide [82]. Leaves of *Nicotiana benthamiana*, including controls and infected leaves, were vacuum-soaked in DAB solutions (2 mg/ mL) for 24 h. Leaves were then transferred into 90% ethanol and boiled until complete decolorization occurred. A hydrogen peroxide kit using the WST-8 method (Grace Biotechnology, China) was used to quantify H_2O_2 content. The absorbance of the supernatant was measured by a spectrophotometer. Three replicates were analyzed for each sample.

Activity measurement of superoxide dismutase

To assess the activities of antioxidant enzymes, systemic leaves from TMV-infected and mock-inoculated plants were collected at 7 dpi. Activity of superoxide dismutase (SOD) was determined using a superoxide dismutase assay kit (Grace Biotechnology, China). Three replicates were analyzed for each sample.

Supplementary Information

The online version contains supplementary material available at https://doi.org/10.1186/s13059-024-03448-8.

Additional file 1. Supplementary figures S1-S6.

Additional file 2. Table S1. Design of crRNAs specific to target genes or viruses. Table S2. Number of transgenic cotton plants containing various Cas13 constructs targeting the *GhCLA* gene. Table S3. Number of transgenic cotton plants containing various Cas13 constructs targeting the *GhPGF* gene. Table S4. Number of transgenic cotton plants containing various Cas13 constructs simultaneously targeting both the *GhCLA* and *GhPGF* genes. Table S5. Number of transgenic tobacco plants containing various Cas13 constructs specifically targeting TRV and TMV, respectively. Table S6. Identification of potential off-target genes associated with *GhCLA* targets. Table S7. Identification of potential off-target genes associated with *GhPGF* targets. Table S8. Primers used in the study.

Additional file 3. Supplementary sequences of the various Cas13 proteins evaluated in this study.

Additional file 4. Review history.

Acknowledgements
The computations presented in this paper were conducted on the bioinformatics computing platform of the National Key Laboratory of Crop Genetic Improvement, Huazhong Agricultural University. We also wish to thank the anonymous peer reviewers for their valuable suggestions to improve the presentation of this research.

Peer review information
Kevin Pang and Wenjing She were the primary editors of this article and managed its editorial process and peer review in collaboration with the rest of the editorial team.

Review history
The review history is available as Additional file 4.

Authors' contributions
J. S., X. Z., and N. X., conceived and designed the experiments. Y. L., performed the experiments and wrote the manuscript. Z. J., A. H., J. R., F. Y., L. J., participated in the experiments. All authors have read and approved the manuscript.

Funding
This work was supported by the Biological Breeding of Stress tolerant and High Yield Cotton Varieties (Project NO.2023ZD04040) to Prof. Ling Min, the Science and Technology Innovation 2030-Major Projects (2023ZD04074, 2022ZD0402001-04) to Prof. Shuangxia Jin and Dr. Zhongping Xu, the National Natural Science Fund of China for Distinguished Young Scholars (32325039), the National Natural Science Fund of China (32272128) and funding from Hubei Hongshan Laboratory (2021hszd013) provided to Prof. Shuangxia Jin.

Data availability
The authors declare that all data supporting the findings of this study are available within the article and its supplementary information files or can be obtained from the corresponding author upon reasonable request. The raw sequencing data generated in this study have been deposited in the National Center for Biotechnology Information (NCBI) Sequence Read Archive (SRA) under project accession number PRJNA1166998 [83]. No custom scripts or software were utilized other than those mentioned in the "Methods" section.

Declarations

Ethics approval and consent to participate
Not applicable.

Competing interests
Shuangxia Jin is an Editorial Board Member for Genome Biology but was not involved in the editorial process of this manuscript.

Received: 12 April 2024 Accepted: 28 November 2024
Published online: 05 December 2024

References

1. McBride JL, Boudreau RL, Harper SQ, Staber PD, Monteys AM, Martins I, Gilmore BL, Burstein H, Peluso RW, Polisky B, et al. Artificial miRNAs mitigate shRNA-mediated toxicity in the brain: implications for the therapeutic development of RNAi. Proc Natl Acad Sci U S A. 2008;105:5868–73.
2. Fire A, Xu S, Montgomery MK, Kostas SA, Driver SE, Mello CC. Potent and specific genetic interference by double-stranded RNA in Caenorhabditis elegans. Nature. 1998;391:806–11.
3. Elbashir SM, Harborth J, Lendeckel W, Yalcin A, Weber K, Tuschl T. Duplexes of 21-nucleotide RNAs mediate RNA interference in cultured mammalian cells. Nature. 2001;411:494–8.
4. Root DE, Hacohen N, Hahn WC, Lander ES, Sabatini DM. Genome-scale loss-of-function screening with a lentiviral RNAi library. Nat Methods. 2006;3:715–9.

5. Jackson AL, Bartz SR, Schelter J, Kobayashi SV, Burchard J, Mao M, Li B, Cavet G, Linsley PS. Expression profiling reveals off-target gene regulation by RNAi. Nat Biotechnol. 2003;21:635–7.
6. Senthil-Kumar M, Mysore KS. Caveat of RNAi in plants: the off-target effect. Methods Mol Biol. 2011;744:13–25.
7. Konermann S, Lotfy P, Brideau NJ, Oki J, Shokhirev MN, Hsu PD. Transcriptome Engineering with RNA-Targeting Type VI-D CRISPR Effectors. Cell. 2018;173:665–76.
8. Smith I, Greenside PG, Natoli T, Lahr DL, Wadden D, Tirosh I, Narayan R, Root DE, Golub TR, Subramanian A, Doench JG. Evaluation of RNAi and CRISPR technologies by large-scale gene expression profiling in the Connectivity Map. PLoS Biol. 2017;15: e2003213.
9. He AT, Liu J, Li F, Yang BB. Targeting circular RNAs as a therapeutic approach: current strategies and challenges. Signal Transduct Target Ther. 2021;6:185.
10. Abudayyeh OO, Gootenberg JS, Konermann S, Joung J, Slaymaker IM, Cox DB, Shmakov S, Makarova KS, Semenova E, Minakhin L, et al. C2c2 is a single-component programmable RNA-guided RNA-targeting CRISPR effector. Science. 2016;353(6299):aaf5573.
11. East-Seletsky A, O'Connell MR, Knight SC, Burstein D, Cate JH, Tjian R, Doudna JA. Two distinct RNase activities of CRISPR-C2c2 enable guide-RNA processing and RNA detection. Nature. 2016;538:270–3.
12. Shmakov S, Smargon A, Scott D, Cox D, Pyzocha N, Yan W, Abudayyeh OO, Gootenberg JS, Makarova KS, Wolf YI, et al. Diversity and evolution of class 2 CRISPR-Cas systems. Nat Rev Microbiol. 2017;15:169–82.
13. Zhang B, Ye Y, Ye W, Perčulija V, Jiang H, Chen Y, Li Y, Chen J, Lin J, Wang S, et al. Two HEPN domains dictate CRISPR RNA maturation and target cleavage in Cas13d. Nat Commun. 2019;10:2544.
14. Zhang B, Ye W, Ye Y, Zhou H, Saeed A, Chen J, Lin J, Perčulija V, Chen Q, Chen CJ, et al. Structural insights into Cas13b-guided CRISPR RNA maturation and recognition. Cell Res. 2018;28:1198–201.
15. Slaymaker IM, Mesa P, Kellner MJ, Kannan S, Brignole E, Koob J, Feliciano PR, Stella S, Abudayyeh OO, Gootenberg JS, et al. High-resolution structure of cas13b and biochemical characterization of RNA targeting and cleavage. Cell Rep. 2021;34: 108865.
16. Shi P, Wu X. Programmable RNA targeting with CRISPR-Cas13. RNA Biol. 2024;21:1–9.
17. Ai Y, Liang D, Wilusz JE. CRISPR/Cas13 effectors have differing extents of off-target effects that limit their utility in eukaryotic cells. Nucleic Acids Res. 2022;50: e65.
18. Wang Q, Liu X, Zhou J, Yang C, Wang G, Tan Y, Wu Y, Zhang S, Yi K, Kang C. The CRISPR-Cas13a Gene-Editing System Induces Collateral Cleavage of RNA in Glioma Cells. Adv Sci (Weinh). 2019;6:1901299.
19. Smargon AA, Cox DBT, Pyzocha NK, Zheng K, Slaymaker IM, Gootenberg JS, Abudayyeh OA, Essletzbichler P, Shmakov S, Makarova KS, et al. Cas13b Is a Type VI-B CRISPR-Associated RNA-Guided RNase Differentially Regulated by Accessory Proteins Csx27 and Csx28. Mol Cell. 2017;65:618–30.
20. Yan WX, Chong S, Zhang H, Makarova KS, Koonin EV, Cheng DR, Scott DA. Cas13d Is a Compact RNA-Targeting Type VI CRISPR Effector Positively Modulated by a WYL-Domain-Containing Accessory Protein. Mol Cell. 2018;70:327–39.
21. Hu Y, Chen Y, Xu J, Wang X, Luo S, Mao B, Zhou Q, Li W. Metagenomic discovery of novel CRISPR-Cas13 systems. Cell Discov. 2022;8:107.
22. Xu C, Zhou Y, Xiao Q, He B, Geng G, Wang Z, Cao B, Dong X, Bai W, Wang Y, et al. Programmable RNA editing with compact CRISPR-Cas13 systems from uncultivated microbes. Nat Methods. 2021;18:499–506.
23. He B, Peng W, Huang J, Zhang H, Zhou Y, Yang X, Liu J, Li Z, Xu C, Xue M, et al. Modulation of metabolic functions through Cas13d-mediated gene knockdown in liver. Protein Cell. 2020;11:518–24.
24. Cox DBT, Gootenberg JS, Abudayyeh OO, Franklin B, Kellner MJ, Joung J, Zhang F. RNA editing with CRISPR-Cas13. Science. 2017;358:1019–27.
25. Abudayyeh OO, Gootenberg JS, Essletzbichler P, Han S, Joung J, Belanto JJ, Verdine V, Cox DBT, Kellner MJ, Regev A, et al. RNA targeting with CRISPR-Cas13. Nature. 2017;550:280–4.
26. Huynh N, Depner N, Larson R, King-Jones K. A versatile toolkit for CRISPR-Cas13-based RNA manipulation in Drosophila. Genome Biol. 2020;21:279.
27. Aman R, Ali Z, Butt H, Mahas A, Aljedaani F, Khan MZ, Ding S, Mahfouz M. RNA virus interference via CRISPR/Cas13a system in plants. Genome Biol. 2018;19:1.
28. Mahas A, Aman R, Mahfouz M. CRISPR-Cas13d mediates robust RNA virus interference in plants. Genome Biol. 2019;20:263.
29. Li L, Liu W, Zhang H, Cai Q, Wen D, Du J, Sun J, Li L, Gao C, Lin P, et al. A New Method for Programmable RNA Editing Using CRISPR Effector Cas13X.1. Tohoku J Exp Med. 2023;260:51–61.
30. Tong H, Huang J, Xiao Q, He B, Dong X, Liu Y, Yang X, Han D, Wang Z, Wang X, et al. High-fidelity Cas13 variants for targeted RNA degradation with minimal collateral effects. Nat Biotechnol. 2023;41:108–19.
31. Xiao Q, Xu Z, Xue Y, Xu C, Han L, Liu Y, Wang F, Zhang R, Han S, Wang X, et al. Rescue of autosomal dominant hearing loss by in vivo delivery of mini dCas13X-derived RNA base editor. Sci Transl Med. 2022;14:eabn0449.
32. Yan Z, Yao Y, Li L, Cai L, Zhang H, Zhang S, Xiao Q, Wang X, Zuo E, Xu C, et al. Treatment of autosomal dominant retinitis pigmentosa caused by RHO-P23H mutation with high-fidelity Cas13X in mice. Mol Ther Nucleic Acids. 2023;33:750–61.
33. Mo J, Chen Z, Qin S, Li S, Liu C, Zhang L, Ran R, Kong Y, Wang F, Liu S, et al. TRADES: Targeted RNA Demethylation by SunTag System. Adv Sci (Weinh). 2020;7:2001402.
34. Yang LZ, Wang Y, Li SQ, Yao RW, Luan PF, Wu H, Carmichael GG, Chen LL. Dynamic Imaging of RNA in Living Cells by CRISPR-Cas13 Systems. Mol Cell. 2019;76:981–97.
35. Zhan X, Zhang F, Zhong Z, Chen R, Wang Y, Chang L, Bock R, Nie B, Zhang J. Generation of virus-resistant potato plants by RNA genome targeting. Plant Biotechnol J. 2019;17:1814–22.
36. Che W, Ye S, Cai A, Cui X, Sun Y. CRISPR-Cas13a Targeting the Enhancer RNA-SMAD7e Inhibits Bladder Cancer Development Both in vitro and in vivo. Front Mol Biosci. 2020;7: 607740.
37. Yin L, Zhao F, Sun H, Wang Z, Huang Y, Zhu W, Xu F, Mei S, Liu X, Zhang D, et al. CRISPR-Cas13a Inhibits HIV-1 Infection. Mol Ther Nucleic Acids. 2020;21:147–55.
38. Aman R, Mahas A, Butt H, Aljedaani F, Mahfouz M. Engineering RNA Virus Interference via the CRISPR/Cas13 Machinery in Arabidopsis. Viruses. 2018;10:732.

39. Zhang W, Jiao Y, Ding C, Shen L, Li Y, Yu Y, Huang K, Li B, Wang F, Yang J. Rapid Detection of Tomato Spotted Wilt Virus With Cas13a in Tomato and Frankliniella occidentalis. Front Microbiol. 2021;12: 745173.
40. Zhang T, Zhao Y, Ye J, Cao X, Xu C, Chen B, An H, Jiao Y, Zhang F, Yang X, Zhou G. Establishing CRISPR/Cas13a immune system conferring RNA virus resistance in both dicot and monocot plants. Plant Biotechnol J. 2019;17:1185–7.
41. Yu Y, Pan Z, Wang X, Bian X, Wang W, Liang Q, Kou M, Ji H, Li Y, Ma D, et al. Targeting of SPCSV-RNase3 via CRISPR-Cas13 confers resistance against sweet potato virus disease. Mol Plant Pathol. 2021;23:104–17.
42. Spencer KP, Burger JT, Campa M. CRISPR-based resistance to grapevine virus A. Front Plant Sci. 2023;14:1296251.
43. Sharma VK, Marla S, Zheng W, Mishra D, Huang J, Zhang W, Morris GP, Cook DE. CRISPR guides induce gene silencing in plants in the absence of Cas. Genome Biol. 2022;23:6.
44. Kelley CP, Haerle MC, Wang ET. Negative autoregulation mitigates collateral RNase activity of repeat-targeting CRISPR-Cas13d in mammalian cells. Cell Rep. 2022;40: 111226.
45. Li Y, Xu J, Guo X, Li Z, Cao L, Liu S, Guo Y, Wang G, Luo Y, Zhang Z, et al. The collateral activity of RfxCas13d can induce lethality in a RfxCas13d knock-in mouse model. Genome Biol. 2023;24:20.
46. Du M, Jillette N, Zhu JJ, Li S, Cheng AW. CRISPR artificial splicing factors Nat Commun. 2020;11:2973.
47. Wang Q, Alariqi M, Wang F, Li B, Ding X, Rui H, Li Y, Xu Z, Qin L, Sun L, et al. The application of a heat-inducible CRISPR/Cas12b (C2c1) genome editing system in tetraploid cotton (G. hirsutum) plants. Plant Biotechnol J. 2020;18:2436–43.
48. Yu L, Li Z, Ding X, Alariqi M, Zhang C, Zhu X, Fan S, Zhu L, Zhang X, Jin S. Developing an efficient CRISPR-dCas9-TV-derived transcriptional activation system to create three novel cotton germplasm materials. Plant Commun. 2023;4: 100600.
49. Qin L, Li J, Wang Q, Xu Z, Sun L, Alariqi M, Manghwar H, Wang G, Li B, Ding X, et al. High-efficient and precise base editing of C•G to T•A in the allotetraploid cotton (Gossypium hirsutum) genome using a modified CRISPR/Cas9 system. Plant Biotechnol J. 2020;18:45–56.
50. Wang P, Zhang J, Sun L, Ma Y, Xu J, Liang S, Deng J, Tan J, Zhang Q, Tu L, et al. High efficient multisites genome editing in allotetraploid cotton (Gossypium hirsutum) using CRISPR/Cas9 system. Plant Biotechnol J. 2018;16:137–50.
51. Ma D, Hu Y, Yang C, Liu B, Fang L, Wan Q, Liang W, Mei G, Wang L, Wang H, et al. Genetic basis for glandular trichome formation in cotton. Nat Commun. 2016;7:10456.
52. Long L, Xu FC, Wang CH, Zhao XT, Yuan M, Song CP, Gao W. Single-cell transcriptome atlas identified novel regulators for pigment gland morphogenesis in cotton. Plant Biotechnol J. 2023;21:1100–2.
53. Li B, Rui H, Li Y, Wang Q, Alariqi M, Qin L, Sun L, Ding X, Wang F, Zou J, et al. Robust CRISPR/Cpf1 (Cas12a)-mediated genome editing in allotetraploid cotton (Gossypium hirsutum). Plant Biotechnol J. 2019;17:1862–4.
54. Wu QW, Kapfhammer JP. The Bacterial Enzyme Cas13 Interferes with Neurite Outgrowth from Cultured Cortical Neurons. Toxins (Basel). 2021;13:262.
55. Wu QW, Kapfhammer JP. The Bacterial Enzyme RfxCas13d Is Less Neurotoxic Than PspCas13b and Could Be a Promising RNA Editing and Interference Tool in the Nervous System. Brain Sci. 2021;11:1054.
56. Kushawah G, Hernandez-Huertas L, Abugattas-Nuñez Del Prado J, Martinez-Morales JR, DeVore ML, Hassan H, Moreno-Sanchez I, Tomas-Gallardo L, Diaz-Moscoso A, Monges DE, et al. CRISPR-Cas13d Induces Efficient mRNA Knockdown in Animal Embryos. Dev Cell. 2020;54:805–17.
57. Zhang C, Konermann S, Brideau NJ, Lotfy P, Wu X, Novick SJ, Strutzenberg T, Griffin PR, Hsu PD, Lyumkis D. Structural Basis for the RNA-Guided Ribonuclease Activity of CRISPR-Cas13d. Cell. 2018;175:212–23.
58. Li R, Fu D, Zhu B, Luo Y, Zhu H. CRISPR/Cas9-mediated mutagenesis of lncRNA1459 alters tomato fruit ripening. Plant J. 2018;94:513–24.
59. Zhou J, Yuan M, Zhao Y, Quan Q, Yu D, Yang H, Tang X, Xin X, Cai G, Qian Q, et al. Efficient deletion of multiple circle RNA loci by CRISPR-Cas9 reveals Os06circ02797 as a putative sponge for OsMIR408 in rice. Plant Biotechnol J. 2021;19:1240–52.
60. Zong Y, Wang Y, Li C, Zhang R, Chen K, Ran Y, Qiu JL, Wang D, Gao C. Precise base editing in rice, wheat and maize with a Cas9-cytidine deaminase fusion. Nat Biotechnol. 2017;35:438–40.
61. Li J, Li H, Chen J, Yan L, Xia L. Toward Precision Genome Editing in Crop Plants. Mol Plant. 2020;13:811–3.
62. Sun Y, Zhang X, Wu C, He Y, Ma Y, Hou H, Guo X, Du W, Zhao Y, Xia L. Engineering Herbicide-Resistant Rice Plants through CRISPR/Cas9-Mediated Homologous Recombination of Acetolactate Synthase. Mol Plant. 2016;9:628–31.
63. Li J, Xu R, Qin R, Liu X, Kong F, Wei P. Genome editing mediated by SpCas9 variants with broad non-canonical PAM compatibility in plants. Mol Plant. 2021;14:352–60.
64. O'Connell MR. Molecular Mechanisms of RNA Targeting by Cas13-containing Type VI CRISPR-Cas Systems. J Mol Biol. 2019;431:66–87.
65. Freije CA, Myhrvold C, Boehm CK, Lin AE, Welch NL, Carter A, Metsky HC, Luo CY, Abudayyeh OO, Gootenberg JS, et al. Programmable Inhibition and Detection of RNA Viruses Using Cas13. Mol Cell. 2019;76:826–37.
66. Wessels HH, Méndez-Mancilla A, Guo X, Legut M, Daniloski Z, Sanjana NE. Massively parallel Cas13 screens reveal principles for guide RNA design. Nat Biotechnol. 2020;38:722–7.
67. Yu L, Alariqi M, Li B, Hussain A, Zhou H, Wang Q, Wang F, Wang G, Zhu X, Hui F, et al: CRISPR/dCas13(Rx) Derived RNA N(6)-methyladenosine (m(6)A) Dynamic Modification in Plant. Adv Sci (Weinh) 2024:e2401118.
68. Li J, Chen Z, Chen F, Xie G, Ling Y, Peng Y, Lin Y, Luo N, Chiang CM, Wang H. Targeted mRNA demethylation using an engineered dCas13b-ALKBH5 fusion protein. Nucleic Acids Res. 2020;48:5684–94.
69. Buchman AB, Brogan DJ, Sun R, Yang T, Hsu PD, Akbari OS. Programmable RNA Targeting Using CasRx in Flies. Crispr j. 2020;3:164–76.
70. Shi P, Murphy MR, Aparicio AO, Kesner JS, Fang Z, Chen Z, Trehan A, Guo Y, Wu X. Collateral activity of the CRISPR/RfxCas13d system in human cells. Commun Biol. 2023;6:334.
71. Webb BA, Chimenti M, Jacobson MP, Barber DL. Dysregulated pH: a perfect storm for cancer progression. Nat Rev Cancer. 2011;11:671–7.
72. Baba M, Kojima K, Nakase R, Imai S, Yamasaki T, Takita T, Crouch RJ, Yasukawa K. Effects of neutral salts and pH on the activity and stability of human RNase H2. J Biochem. 2017;162:211–9.

73. Parks SK, Chiche J, Pouysségur J. Disrupting proton dynamics and energy metabolism for cancer therapy. Nat Rev Cancer. 2013;13:611–23.
74. Tng PYL, Carabajal Paladino L, Verkuijl SAN, Purcell J, Merits A, Leftwich PT, Fragkoudis R, Noad R, Alphey L. Cas13b-dependent and Cas13b-independent RNA knockdown of viral sequences in mosquito cells following guide RNA expression. Commun Biol. 2020;3:413.
75. Li B, Liang S, Alariqi M, Wang F, Wang G, Wang Q, Xu Z, Yu L, Naeem Zafar M, Sun L, et al. The application of temperature sensitivity CRISPR/LbCpf1 (LbCas12a) mediated genome editing in allotetraploid cotton (G. hirsutum) and creation of nontransgenic, gossypol-free cotton. Plant Biotechnol J. 2021;19:221–3.
76. Wang G, Xu Z, Wang F, Huang Y, Xin Y, Liang S, Li B, Si H, Sun L, Wang Q, et al. Development of an efficient and precise adenine base editor (ABE) with expanded target range in allotetraploid cotton (Gossypium hirsutum). BMC Biol. 2022;20:45.
77. Li J, Wang M, Li Y, Zhang Q, Lindsey K, Daniell H, Jin S, Zhang X. Multi-omics analyses reveal epigenomics basis for cotton somatic embryogenesis through successive regeneration acclimation process. Plant Biotechnol J. 2019;17:435–50.
78. Sun L, Alariqi M, Zhu Y, Li J, Li Z, Wang Q, Li Y, Rui H, Zhang X, Jin S. Red fluorescent protein (DsRed2), an ideal reporter for cotton genetic transformation and molecular breeding. The Crop Journal. 2018;6:366–76.
79. Withanage MHH, Liang H, Zeng E. RNA-Seq Experiment and Data Analysis. Methods Mol Biol. 2022;2418:405–24.
80. Arnon DI. COPPER ENZYMES IN ISOLATED CHLOROPLASTS. POLYPHENOLOXIDASE IN BETA VULGARIS Plant Physiol. 1949;24:1–15.
81. Smith FH. Determination of gossypol in leaves and flower buds of Gossypium. J Am Oil Chem Soc. 1967;44:267–9.
82. Daudi A, O'Brien JA. Detection of Hydrogen Peroxide by DAB Staining in Arabidopsis Leaves. Bio Protoc. 2012;2:e263.
83. Yu L, Zhou J, Amjad H, Jia R, Fan Y, Liu J, Nie X, Zhang X, Jin S: Systemic evaluation of various CRISPR/Cas13 orthologs for knockdown of targeted transcripts in plants. *BioProject* 2024, https://www.ncbi.nlm.nih.gov/bioproject/PRJNA1166998.

Publisher's Note